5 DESIGN OF SPINDLES AND SPINDLE SUPPORTS

5.1 FUNCTIONS OF SPINDLE UNIT AND REQUIREMENTS

Functions The spindle unit of a machine tool performs the following important functions:

1. Centreing the workpiece, e.g., in lathes, turrets, boring machines, etc., or the cutting tool, as in drilling and milling machines.
2. Clamping the workpiece or cutting tool, as the case may be, such that the workpiece or cutting tool is reliably held in position during the machining operation.
3. Imparting rotary motion (e.g., in lathes) or rotary cum translatory motion (e.g., in drilling machines) to the cutting tool or workpiece.
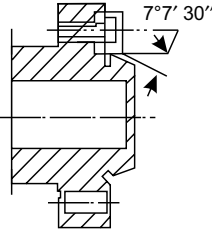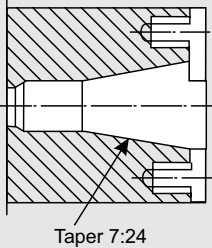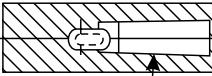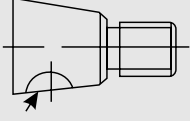
The operational capabilities of a machine tool in terms of productivity as well as accuracy and finish of machined parts largely depend upon the extent to which these functions are qualitatively satisfied. They also determine the important design requirements to spindle units which are listed below.

Requirements

1. The spindle should rotate with a high degree of accuracy. The accuracy of rotation is determined by the radial and axial run out of the spindle nose, and these must not exceed certain permissible values which are specified depending on the required machining accuracy. The rotational accuracy is influenced maximum by the stiffness and accuracy of spindle bearings, particularly the one located at the front end.
2. The spindle unit must have high static stiffness. The stiffness of the unit is made up of the stiffness of the spindle unit proper and the spindle bearings. Machining accuracy is influenced by bending, axial as well as torsional stiffness.
3. The spindle unit must have high dynamic stiffness and damping. Poor dynamic stability of the spindle unit adversely affects the dynamic behaviour of the machine tool as a whole, resulting in poor surface finish and loss of productivity due to restriction on the limiting undeformed width of cut.
4. The mating surfaces that are liable to wear restrict the life of the spindle unit. These surfaces, such as journals, quills (in drilling machines), etc., must be hardened to improve their wear resistance. The spindle bearings must also be selected or designed to retain the initial accuracy during the service life of the machine tool.
5. The deformation of the spindle due to heat transmitted to it by the bearings, cutting tool, work piece, etc., should not be large, as this has an adverse effect on the machining accuracy. In case of spindles running at high rotational speeds, particular care should be taken in selecting or designing the front bearing as it is the major source of heat transmitted to the spindle.
6. The spindle unit must have a fixture which provides quick and reliable centreing and clamping of the cutting tool or workpiece. The centreing is achieved by means of an external or internal taper at the

front end of the spindle. The spindle ends, including the taper have been standardised for the common groups of machine tools and are shown in Table 5.1.

Table 5.1   *Spindle ends*

S. No.	Figure	Application	Remark
1.	7°7′ 30″	Lathes, turrets, single spindle automatic and semi-automatic lathes, etc.	External taper 7°7′30″ is used only in heavy-duty machine tools for centreing chuck or face plate. Generally, chucks or face plates are centred by a cylindrical surface.
2.	Taper 7:24	Milling machines	Steep taper 7 : 24 is necessary so that the milling arbor and cutter once located and clamped should be able to hold their position under the pulsating milling force.
3.	Morse taper	Drilling and boring machines	Morse tapers come in 8 sizes identified as MT0-MT7. Taper angle varies between 1°25′27″ and 1°30′26″. Small taper is essential as rotation is transmitted from the spindle to the drill shank by friction.
4.	Taper 1:3	Grinding machines	In grinding machines, the con-centricity of location is extremely important. Therefore, the grinding wheel is mounted on an adaptor which is press-fitted on the spindle taper.

5.2   MATERIALS OF SPINDLES

The blank for a machine tool spindle may be

1. rolled stock in the case of spindles having diameter < 150 mm, and

2. casting (preferably obtained by centrifugal casting method) in the case of spindles having diameter > 150 mm.

It should be borne in mind that if the spindle blank is cut from rolled stock, the cutting must be done by a cutting tool (shears, rotary saw, parting tool, etc.) to avoid additional distortions of the material microstructure.

In machine tool spindle design, the critical design parameter is not strength but stiffness. If we compare the mechanical properties of various steels, we find that their modulus of elasticity is more or less equal, although the strength of alloyed steels can be considerably greater than that of mild steel. Since stiffness (the main design parameter) is primarily determined by the modulus of elasticity of the material, it may be concluded that no particular benefit accrues from using costly alloyed steels for making spindles.

In the light of the preceding discussion and the requirements laid down in Sec. 5.1, the following recommendations for selecting the spindle material may be formulated

1. for normal accuracy spindles, plain carbon steels **C45** and **C59** (A_iS_i C1045 and C1050) hardened and tempered to $RC = 30$.
2. for above normal accuracy spindles—low alloy steel 40 **Cr** 1 **Mn** *60* **Si** *27* **Ni**25 (A_iS_i 5140) induction hardened to $RC = 50$–56; if induction hardening of above normal accuracy spindles is difficult due to complex profile then low alloy steel 50 **Cr** 1 **Mn** *60* **Si** *27* **Ni** *25* (A_iS_i 5147) is used with hardening to $RC = 55$–60.
3. for spindles of precision machine tools, particularly those with sliding bearings—low alloyed steel 20 **Cr** 1 **Mn** *60* **Si** *27* **Ni** *25* (A_iS_i 5120) case hardened to $RC = 56$–60 or 38 **Cr** 1 **A1** *90* **Mn** *45* **Si** *27* **Ni** *25* **Mo** 20 (EN 41) nitrided to $RC = 63$–68, and
4. for hollow, heavy-duty spindles—grey cast iron or, spheroidal graphite iron.

5.3 EFFECT OF MACHINE TOOL COMPLIANCE ON MACHINING ACCURACY

Consider a uniform shaft being machined between centres on a lathe (Fig. 5.1). Let K_A be the stiffness of centre A and K_B that of centre B. Due to radial component P_y of the cutting force, centre A will be displaced by a distance

$$y_A = \frac{P_A}{K_A} \qquad (5.1)$$

and centre B by

$$y_B = \frac{P_B}{K_B} \qquad (5.2)$$

Fig. 5.1 *Schematic diagram of a simple turning operation*

Here P_A and P_B are the forces of reaction at ends A and B, respectively. They can be determined from the following equations of static equilibrium:

1. **Moment of Forces about Point** $B = 0$, i.e.,
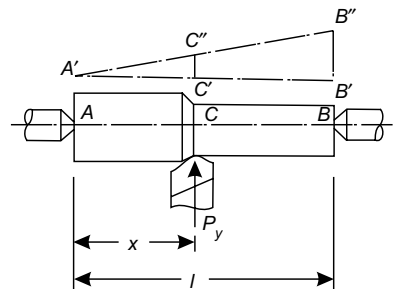
$$P_A l = P_y (l - x)$$

wherefrom,

$$P_A = P_y\left(1 - \frac{x}{l}\right) \tag{5.3}$$

2. **Moment of Forces about Point** $A = 0$, i.e.,

$$P_B \cdot l = P_y \cdot x$$

wherefrom,

$$P_B = P_y \frac{x}{l} \tag{5.4}$$

Substituting the values of P_A and P_B in Eqs (5.1) and (5.2), respectively, we obtain

$$y_A = P_y\left(1 - \frac{x}{l}\right)\frac{1}{K_A} \tag{5.5}$$

$$y_B = P_y \cdot \frac{x}{l}\frac{1}{K_B} \tag{5.6}$$

Owing to the compliance of centres A and B, the workpiece occupies position $A'B''$ (assuming $K_A > K_B$) and its displacement at the cutting point can be found as

$$y_x = y_A + C'C''$$

from similar triangles $A'C'C''$ and $A'B'B''$, we have

$$\frac{C'C''}{B'B''} = \frac{x}{l}$$

since

$$B'B'' = y_B - y_A$$

$$C'C'' = (y_B - y_A)\frac{x}{l}$$

Therefore,

$$y_x = y_A + (y_B - y_A)\frac{x}{l} \tag{5.7}$$

Substituting the values of y_A and y_B from Eqs (5.5) and (5.6), Eq. (5.7) yields

$$y_x = P_y\left[\left(1 - \frac{x}{l}\right)\cdot\frac{1}{K_A} + \frac{x}{l}\left\{\frac{x}{l}\cdot\frac{1}{K_B} - \left(1 - \frac{x}{l}\right)\frac{1}{K_A}\right\}\right]$$

or

$$y_x = \frac{P_y}{K_A \cdot K_B}\left[K_B\left(1 - \frac{x}{l}\right)^2 + K_A\left(\frac{x}{l}\right)^2\right] \tag{5.8}$$

If it is assumed that $K_A/K_B = \alpha$, Eq. (5.8) can be modified as follows:

$$y_x = \frac{P_y}{K_A}\left[\left(1 - \frac{x}{l}\right)^2 + \alpha\left(\frac{x}{l}\right)^2\right] \tag{5.9}$$

wherefrom, keeping in mind that $P_y/K_A = y_{A\,max}$, we get

$$\frac{y_x}{y_{A\,max}} = \left(1 - \frac{x}{l}\right)^2 + \alpha\left(\frac{x}{l}\right)^2 \tag{5.10}$$

The variation of $y_x/y_{A\,max}$ plotted as a function of x/l for different values of α is depicted in Fig. 5.2. From the curves it may be concluded that

1. when $\alpha < 1$, i.e., stiffness of the headstock centre is less than the stiffness of the tailstock centre, maximum displacement of the workpiece occurs at the headstock; and
2. when $\alpha > 1$, i.e., the stiffness of the tailstock centre is less than that of the headstock, maximum displacement of the workpiece occurs at the tailstock.
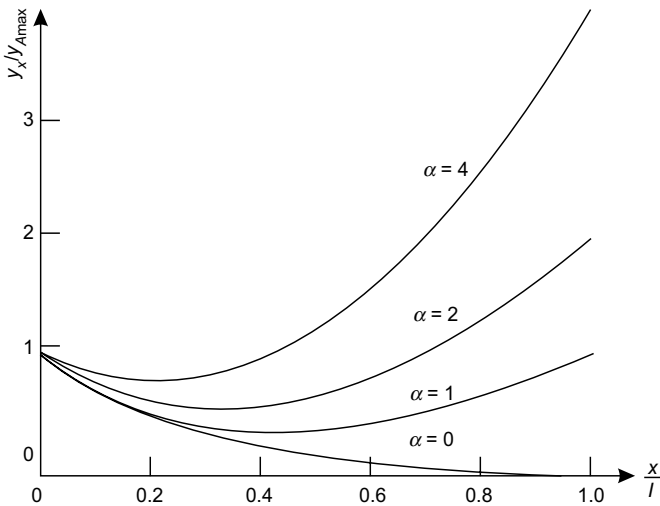

Fig. 5.2 *Variation of y_x/y_{Amax} as a function of x/l*

The deviation of the profile of a turned job from a true cylinder depends upon the difference of maximum and minimum displacements of the workpiece axis. As already stated, maximum displacement occurs at the headstock or tailstock depending upon the value of α.

The deflection is minimum where compliance y_x/P_y is minimum. Therefore, the location of the point of minimum deflection may be determined from the condition

$$\frac{d}{dx}\left(\frac{y_x}{P_y}\right) = 0$$

From Eq. (5.9),

$$\frac{d}{dx}\left(\frac{y_x}{P_y}\right) = \frac{1}{K_A}\left(\frac{2x}{l^2} - \frac{2}{l}\right) + \frac{1}{K_B}\frac{2x}{l^2}$$

which, upon equating to zero yields

$$x_0 = \frac{K_B \cdot l}{K_A + K_B} \tag{5.11}$$

That the deflection at x_0 is minimum (and not maximum) is confirmed from the fact that

$$\frac{d^2}{dx^2}\left(\frac{y_x}{P_y}\right) = \frac{2}{l^2}\left(\frac{1}{K_A} + \frac{1}{K_B}\right) > 0$$

Substituting the value of x_0 in Eq. (5.10), we obtain

$$y_{\min} = \left[\left(1 - \frac{K_B}{K_A + K_B}\right)^2 + \alpha\left(\frac{K_B}{K_A + K_B}\right)^2\right] y_{A\max}$$

or

$$y_{\min} = \frac{\alpha}{1 + \alpha} y_{A\max} \tag{5.12}$$

For $\alpha < 1$: The maximum displacement occurs at the headstock centre, i.e., $y_{\max} = y_{A\max}$. Therefore,

$$y_{\max} - y_{\min} = y_{A\max} - \frac{\alpha}{1+\alpha} \cdot y_{A\max}$$

wherefrom,

$$\frac{y_{\max} - y_{\min}}{y_{A\max}} = \frac{1}{1+\alpha} \tag{5.13}$$

For $\alpha > 1$: The maximum displacement occurs at the tailstock centre, i.e., $y_{\max} = y_{B\max}$. Therefore,

$$y_{\max} - y_{\min} = y_{B\max} - \frac{\alpha}{1+\alpha} \cdot y_{A\max} = y_{A\max}\left[\frac{y_{B\max}}{y_{A\max}} - \frac{\alpha}{1+\alpha}\right]$$

as $y_{B\max}/y_{A\max} = K_A/K_B = \alpha$, we get

$$\frac{y_{\max} - y_{\min}}{y_{A\max}} = \frac{\alpha^2}{1+\alpha} \tag{5.14}$$

It should be noted that the profile accuracy is governed by Eq. (5.13) for $\alpha < 1$ and by Eq. (5.14) for $\alpha > 1$. The relationships represented by Eqs (5.13) and (5.14) have been plotted as functions of α and shown in Fig. 5.3. The dotted portions of the curve represent the range in which the curves are not valid.

It is evident from Fig. 5.3 that the difference $y_{\max} - y_{\min}$ is minimum at $\alpha = 1$ and is equal to half the headstock centre displacement, i.e.,

$$(y_{\max} - y_{\min})_{\min} = \frac{y_{A\max}}{2} \tag{5.15}$$

It may thus be concluded that the maximum profile accuracy is achieved when the stiffness of headstock and tailstock centre are equal.
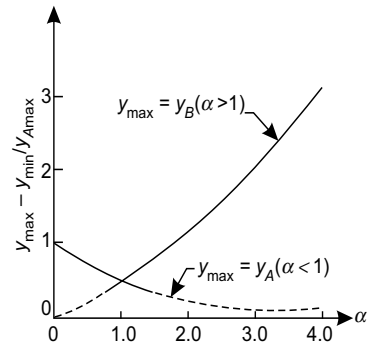

Fig. 5.3 *Variation of* $\dfrac{y_{\max} - y_{\min}}{y_{A\max}}$ *as a function of* α

If the stiffness of the saddle is given by K_s, the displacement of the cutting edge due to saddle compliance can be found as

$$y_s = \frac{P_y}{K_s}$$

The total compliance of the machine tool can be found as the sum of compliances of the workpiece and saddle, i.e.,

$$C_{mt} = \frac{y_{mt}}{P_y} = \frac{y_s}{P_y} + \frac{y_x}{P_y}$$

or

$$C_{mt} = \frac{1}{K_s} + \frac{1}{K_A}\left(1 - \frac{x}{l}\right)^2 + \frac{1}{K_B}\left(\frac{x}{l}\right)^2 \qquad (5.16)$$

The machining accuracy which includes both profile as well as dimensional accuracy is determined by the machine tool compliance as expressed through Eq. (5.16). The representative total compliance values for some machine tools are given in Table 5.2.

Table 5.2 *Values of compliance C_{mt} for different machine tools*

S. No.	Machine tool	Description	Compliance (micron/kgf)
1.	Lathe, workpiece clamped between centres	Height of centres 200 mm Height of centres 300 mm Height of centres 400 mm	0.75 0.52 0.38
2.	Lathe, workpiece clamped in chuck which is screwed on spindle nose	Height of centres 200 mm Height of centres 300 mm	1.5 1.2
3.	Multiple-spindle vertical, semiautomatic lathes	Height of centres 400 mm	0.5–0.7
4.	Automatic bar lathes	Screw type Multiple-spindle type	0.2–0.3 0.3–0.4
5.	Vertical milling machine	Drive motor rating = 7 kW Table size 320 × 1250 mm	0.4
6.	Plano-milling machine	Table size 4.25 × 1.5 m	0.4
7.	Vertical turning and boring mill	Table diameter 3 m	0.36
8.	Centreless grinding machine		1.00

5.4 DESIGN CALCULATIONS OF SPINDLES

Figure 5.4 shows the schematic diagram of a spindle. As is evident from the diagram, the spindle represents a shaft with

1. supported length l acted upon by driving force P_2, and
2. cantilever of length c acted upon by external force P_1.

The spindle is basically designed for bending stiffness which requires that the maximum deflection of the spindle nose should not exceed a certain pre specified value, i.e.,
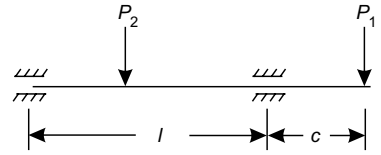
$$y_{max} \leq [y] \qquad (5.17)$$

The total deflection of the spindle nose consists of

Fig. 5.4 *Schematic diagram of a spindle*

1. deflection y_1 of the spindle axis due to bending forces P_1 and P_2, and
2. deflection y_2 of the spindle axis due to compliance of the spindle supports.

When the spindle has a tapered hole in which a centre or cutting tool is mounted, the total deflection of the centre or cutting tool consists of deflections (1) and (2) above in addition to

3. deflection y_3 of the centre or cutting tool due to compliance of the tapered joint.

5.4.1 Deflection of Spindle Axis due to Bending

For determining the deflection of the spindle nose due to bending, we must first establish a proper design diagram. In this context, the following guidelines may be employed with success:

1. If the spindle is supported on a single anti-friction bearing at each end, it may be represented as a simply supported beam.
2. If the spindle is supported in a sleeve bearing, the supported journal is analysed as a beam on an elastic foundation; for purposes of the design diagram the sleeve bearing is replaced by a simple hinged support and a reactive moment M_r acting at the middle of the sleeve bearing.

The reactive moment is given as

$$M_r = k \cdot M$$

where M = bending moment at the support,
k = coefficient which varies from $k = 0$ at small loads to $k = 0.3$–0.35

Consider, for example, the spindle shown schematically in Fig. 5.5a. By replacing the rear ball bearing by a hinge, and the front sleeve bearing by a hinge and reactive moment M_r, the spindle can be reduced to the design diagram of Fig. 5.5b. The deflection at the free end of the beam (spindle nose) can be determined by Macaulay's method and is found to be

$$y_1 = \frac{1}{3EI} \left[p_1 c^2 (l + c) - 0.5 P_2 abc \left(1 - \frac{a}{l} \right) + M_r lc \right] \quad (5.18)$$

where E = modulus of elasticity of the spindle material
I = average moment of inertia of the spindle section

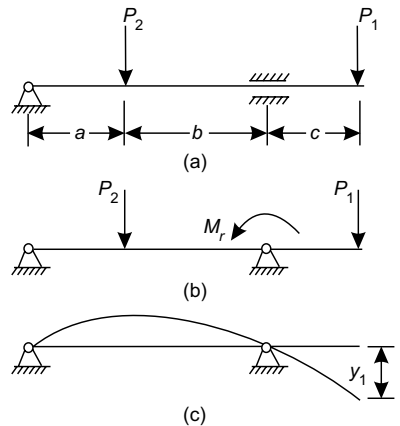The deflected beam is shown at Fig. 5.5c.

Fig. 5.5 *(a) Schematic diagram of the spindle (b) Design diagram of the spindle (c) Deflected axis of the spindle*

5.4.2 Deflection of Spindle Axis due to Compliance of Spindle Supports

Let δ_A and δ_B represent the displacement of the rear and front supports, respectively. Owing to the compliance of supports, the spindle deflects as shown in Fig. 5.6 (for design purposes we are considering the most unfavourable case when bearing displacements are oppositely directed). From similar triangles OCC' and OBB',

$$\frac{y_2}{c+x} = \frac{\delta_B}{x}$$

Fig. 5.6 *Deflection of spindle due to compliance of the supports*

wherefrom,

$$y_2 = \left(1 + \frac{c}{x}\right)\delta_B \tag{5.19}$$

Again, from similar triangles OAA' and OBB',

$$\frac{\delta_B}{x} = \frac{\delta_A}{l-x}$$

wherefrom,

$$x = \frac{l \cdot \delta_B}{\delta_A + \delta_B} \tag{5.20}$$

Substituting this value of x in Eq. (5.19), we get

$$y_2 = \delta_B\left(1 + \frac{C}{l}\right) + \delta_A\frac{c}{l} \tag{5.21}$$

It is evident from Eq. (5.21) that displacement δ_B of the front bearing has greater influence upon deflection y_2 of spindle nose than displacement δ_A of the rear bearing.

Displacements δ_A and δ_B can be determined from the following expressions:

$$\delta_A = \frac{R_A}{K_A} \tag{5.22}$$

$$\delta_B = \frac{R_B}{K_B} \tag{5.23}$$

where R_A and R_B are reactions at supports A and B, respectively, while K_A and K_B is their respective stiffness.

Reactions R_A and R_B can be found from the following equilibrium conditions applied to the design diagram of Fig. 5.5b:

1. **Moment of All Forces about Point** $A = 0$, i.e.,

$$\Sigma M_A = 0 \quad \text{or} \quad R_B \cdot l - P_2 \cdot a + M_r - P_1(c + l) = 0$$

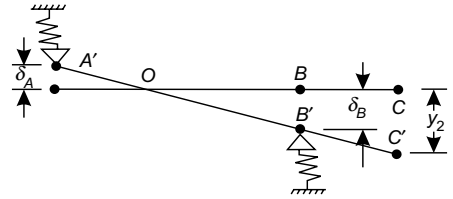wherefrom,

$$R_B = \frac{P_2 a - M_r + P_1(l + c)}{l} \tag{5.24}$$

2. **Moment of All Forces about Point** $B = 0$, i.e.,

$$\Sigma M_B = 0 \quad \text{or} \quad R_A \cdot l - P_2 \cdot b - M_r + P_1 c = 0$$

wherefrom,

$$R_A = \frac{P_2 b + M_r - P_1 c}{l} \tag{5.25}$$

Keeping in mind Eqs (5.22)–(5.25), the final expression for deflection y_2 may be written as follows:

$$y_2 = \frac{P_2 a - M_r + P_1(l + c)}{l \cdot K_B}\left(1 + \frac{c}{l}\right) + \frac{P_2 b + M_r - P_1 c}{l \cdot K_A} \times \frac{c}{l} \tag{5.26}$$

The total deflection of the spindle nose can be determined as the sum of y_1 (Eq. (5.18)) and y_2 (Eq. (5.26)), i.e.,

$$y = y_1 + y_2 \tag{5.26a}$$

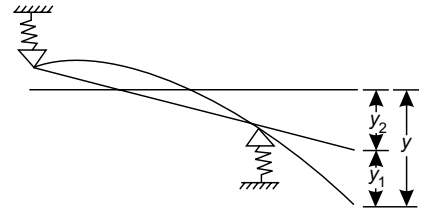The resultant deflected axis of the spindle is shown in Fig. 5.7.

Fig. 5.7 *Total deflection of the spindle axis*

5.4.3 Optimum Spacing between Spindle Supports

An important parameter in spindle design is the ratio $\lambda = l/c$. The optimum value of this ratio is the one that ensures minimum total deflection y; it can be determined from the condition $dy/d\lambda = 0$.

The qualitative variations of y_1, y_2 and $y_1 + y_2$, for constant values of forces P_1 and P_2 are depicted in Fig. 5.8 as functions of ratio l/c.

The point of minimum of the $y_1 + y_2$ curve yields the optimum value of ratio l/c which generally lies between 3 and 5. The value of λ_{opt} depends upon

1. ratio

$$\alpha = \frac{K_B}{K_A}$$

of the stiffness of the front and rear bearings, and

2. factor

$$F = \frac{K_B}{K_c} \frac{I_c}{I_t}$$

where $K_c = \dfrac{3EI_c}{c^3}$ = bending stiffness of the cantilever,

Fig. 5.8 *Effect of l/c ratio on y_1, y_2 and $y_1 + y_2$*

I_c = average moment of inertia of the spindle over the cantilever length, and

I_l = average moment of inertia of the spindle over the supported length.
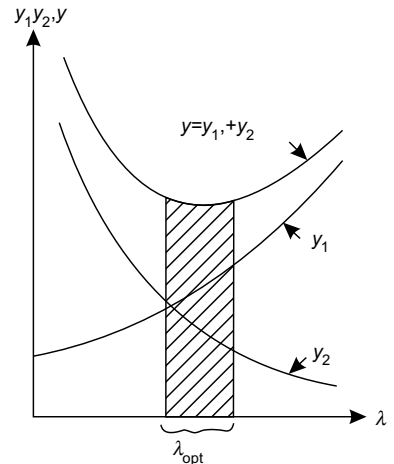
The variation of λ_{opt} as a function of F is depicted in Fig. 5.9 for $\alpha = 1$ and $\alpha = 10$.

When the spindle is mounted on anti-friction bearings, an additional check is necessary to ensure that the constraint $\lambda_{opt} \geq \lambda_{min} = 2.5$ is not violated because for $\lambda < 2.5$ the bearing play leads to considerable radial run out of the spindle nose.

An opposite constraint on maximum span stems from the requirement that for normal functioning of the spindle driving gear, the stiffness of the span should not be less than 25–50 kgf/micron. This constraint is expressed through the following relationship:

$$l \leq \frac{D_l^{4/3}}{k^{1/3}} \tag{5.27}$$

Fig. 5.9 *Effect of spindle and supports stiffness on l_{opt}*

where D_l = average diameter of the supported length of the spindle

$k = 0.05$ in the case of normal accuracy machine tools and 0.1 for precision machine tools

When the spindle is supported on hydrostatic journal bearings, the maximum deflection at the middle of the span should satisfy the condition,

$$y_{l\,max} \leq 10^{-4}l \tag{5.28}$$

and the maximum span length l_{max} should be limited by the above constraint. This constraint is based upon the requirement that the maximum misalignment due to deflection of the journals should not exceed one-third of the bearing gap.

5.4.4 Deflection due to Compliance of the Tapered Joint

The spindle ends of most machine tools have a tapered hole for accommodating a centre (as in lathes) or cutting tool shank (as in milling and drilling machines). The deflection of the shank or centre at a distance d from the spindle axis (Fig. 5.10), where a force P is acting, may be represented as[1]

$$y_3 = \delta + \theta d \tag{5.29}$$

Fig. 5.10 *Schematic diagram of a tapered joint*

where δ = displacement of the shank or centre at the edge of taper due to contact compliance and

θ = angle of slope of the shank or centre at the edge of the taper

If the manufacturing errors of the taper are ignored, δ and θ can be determined from the following expressions:

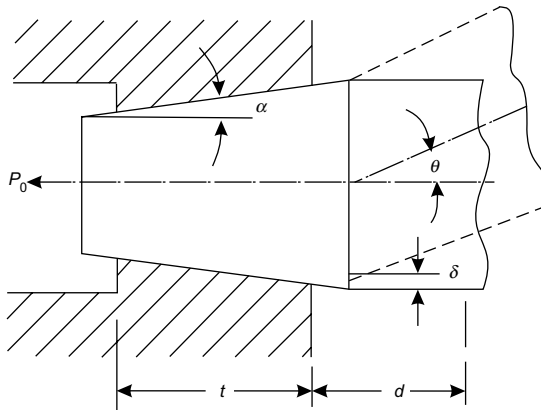$$\delta = \frac{4D\beta C_1}{\pi D}(\beta dC_2 + C_3) \text{ micron} \tag{5.30}$$

$$\theta = \frac{4P\beta^2 C_1}{\pi D}(2\beta dC_4 + C_2) \tag{5.31}$$

In these expressions,

C_1 = coefficient of contact compliance; for Morse tapers $C_1 = 0.03$–0.06, while for the 7 : 24 taper $C_1 = 0.02$ micron cm^2/kgf

C_2, C_3, C_4 = coefficients that account for the diameter variation along the length of taper; for Morse tapers $C_2 = C_3 = C_4 = 1$, while for the 7 : 24 taper $C_2 = C_3 = 1.35$ and $C_4 = 1$

$$\beta = \left(\frac{1}{2.3C_1 D^4}\right)^{1/4} \text{cm}^{-1}$$

D and d are expressed in cm

Generally, displacement δ due to contact compliance can be ignored in comparison with the displacement due to bending of the shank or centre. The expression for y_3 can then be written as

$$y_3 = \frac{4P\beta^2 C_1}{\pi D}(2\beta dC_4 + C_2)d \text{ micron} \tag{5.32}$$

If it is assumed that $2\beta dC_4$ is much greater than C_2 (which is true), the following simplified expression for y_3 is obtained:

$$y_3 = 2.55\frac{Pd^2}{D}\beta^3 C_1 C_4 \text{ micron} \tag{5.33}$$

Keeping in mind the expression for β and substituting $C_4 = 1$ and $C_1 = 0.02$ micron·cm^2/kgf, the expression for displacement of a shank or centre mounted in a 7 : 24 taper can be written as follows:

$$y_3 = \frac{Pd^2}{2D^4} \text{ micron} \tag{5.34}$$

Consequently, the stiffness of the 7 : 24 taper can be written as

$$K_{7:24} = \frac{P}{y_3} = \frac{2D^4}{d^2} \frac{\text{kgf}}{\text{micron}} \tag{5.35}$$

As the d/D ratio increases, the stiffness of the tapered joint decreases.

Equation (5.34) has been derived on the assumption that manufacturing errors of the taper are negligible. As a matter of fact, any difference in the taper angle of the hole and shank severely affects the stiffness of the tapered joint. A difference of 30–40' in taper angles can easily reduce the stiffness of a 7 : 24 taper by 10–15 times. The difference in taper angles should normally not exceed 1' and the shank should have the larger taper angle.

The centring accuracy can be considerably improved and the stiffness of the tapered joint significantly raised by applying an axial tightening force on the centre or shank. The tightening force should be such as to produce a pressure of $p = 15$–25 kgf/cm^2 on the tapered surfaces. The required magnitude of the tightening force can be determined from the expression,

$$P_0 = p \cdot \pi(D - t \tan \alpha) \cdot t \tan (\alpha + \rho) \tag{5.36}$$

where ρ = angle of friction, generally $\rho = 12$–$14°$

D and t are expressed in cm

In large machine tools mechanical tightening devices must be employed to

1. provide large tightening force which is difficult to obtain manually, and
2. ensure that the larger tightening force is not transmitted to the thrust bearings of the spindle.

The principle of operation of such a device may be explained with the help of Fig. 5.11.[2] The device consists of bolt 2 screwed into tapered shank 1, spring-loaded levers 3, pulling rod 4, strong spring-loaded helical spring 5 and hydraulic cylinder 6 (Fig. 5.11a). When the hydraulic cylinder applies pressure, spring 5 is compressed, rod 4 occupies the lowered position and levers 3 are tilted inwards due to the pressure of spring 7 (Fig. 5.11b). The cutting tool (e.g., face milling cutter) assembled on the adaptor with a tapered shank is now introduced in the spindle hole. A slight upward push on the shank is sufficient to overcome the resistance of springs 7 and open the levers, which engulf the bolt head. The shank now hangs freely, supported by the levers.

For tightening the shank, the pressure of the hydraulic cylinder is released. Consequently, spring 5 begins to expand; pulling rod 4 upwards. The tapered shank is also pulled upwards and tightened inside the tapered hole. This position is shown in Fig. 5.11c.
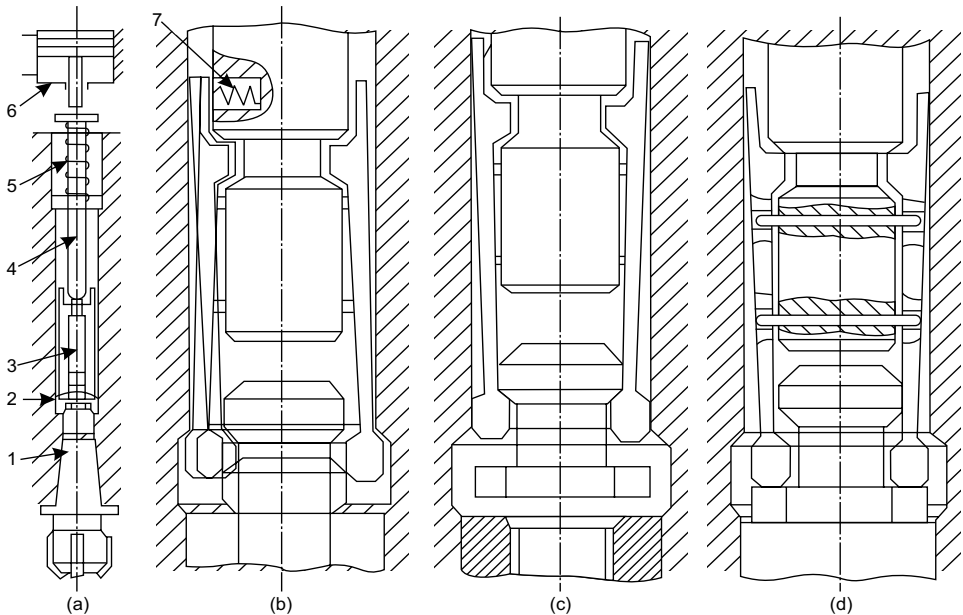

Fig. 5.11 *Schematic diagram of a quick acting mechanical tightening device*

For unloosening the shank, rod 3 is pushed downwards by means of the hydraulic cylinder. In their downward movement the levers push at the face of the tapered shank and unloosen it. The downward movement of rod 3 is stopped immediately as the shank becomes free. The shank along with the cutting tool now again hangs freely, supported only by spring-loaded levers. It can be easily removed from the spindle by a slight downward pull of the hand.

This mechanised device not only serves the two functions listed above but has the added advantage of being quick-acting (changing time is of the order of 5–6 s). Due to all these factors, it is finding wide application in numerically controlled milling machines with automatic tool change provision. In some designs, a collet is used instead of spring-loaded levers and a packet of leaf springs in place of spring 5.

5.4.5 Permissible Deflection and Design for Stiffness: Additional Check for Strength

Having calculated deflection components y_1, y_2 and y_3 from Eqs (5.18), (5.26) from (5.32), respectively, the total deflection of the spindle nose can be found as the sum of the three. The design for stiffness can then be carried out in accordance with Eq. (5.17). The permissible deflection of the spindle nose $[y]$ depends upon the machining accuracy required of the machine tool being designed. In general, it should be less than one-third of the maximum permissible tolerance on radial run out of the spindle nose.

Machining accuracy depends not only upon the radial stiffness of the spindle, but also upon its axial and torsional stiffness.

The axial displacement of the spindle unit consists of the axial deformation of the spindle plus the deformation of the spindle thrust bearings. For a majority of machine tools, the latter component is predominant. Therefore, the axial run out of the spindle can be kept within reasonable limits only by a proper selection of the thrust bearings.

The torsional stiffness of machine tool spindles significantly influences the machining accuracy in metal-removal operations, such as gear and thread cutting in which the feed and primary cutting motions are kinematically linked. The torsional deformation of the spindle unit consists of the deformation of the spindle proper plus the deformation of the drive components. Generally, the first component can be ignored in the design calculations.

As stated earlier in Sec. 5.4, spindles are designed for stiffness, primarily radial. However, in heavily loaded spindles the stiffness design must be substantiated by a strength check against fatigue failure. The strength check requires that

$$n \geq n_{\min} \tag{5.37}$$

where n = factor of safety against fatigue failure

$n_{\min}$ = minimum value of safety factor, generally equal to 1.3 to 1.5

For spindles subjected to combined bending and torsion, the factor of safety n is calculated from the expression,

$$n = \frac{(1 - \alpha^4) d_e^3 \sigma_{-1}}{10\sqrt{(aM_b)^2 + (bM_t)^2}} \tag{5.38}$$

where $\alpha = d_i/d_e$ = ratio of the internal diameter to the external; d_e is in cm

σ_{-1} = endurance limit of the spindle material, kgf/cm^2

M_b = mean value of the bending moment acting on the spindle, kgf · cm

M_t = mean value of the torque acting on the spindle, kgf · cm

a = coefficient that accounts for the variation of bending moment and stress concentration

b = coefficient that accounts for the variation of torque and stress concentration

Coefficient a can be determined from the following expression:

$$a = K_\sigma(1 + C) \tag{5.39}$$

where K_σ = dynamic stress concentration coefficient for normal stresses, generally K_σ = 1.7–2

$C = M_{ba}/M_b$ = ratio of amplitude of the bending moment to its average value

Coefficient b can be calculated from the following formula:

$$b = \frac{\sigma_{-1}}{\sigma_y} + K_\tau C_t \tag{5.40}$$

where σ_y = yield stress of the spindle material, kgf/cm^2

k_τ = dynamic stress concentration coefficient for shearing stress, generally K_τ = 1.7–2

$C_t = M_{ta}/M_t$ = ratio of amplitude of torque to its average value

The values of C and C_t in Eqs (5.39) and (5.40), respectively depend upon the machining conditions. For instance, in a super finishing operation there is virtually no variation of the bending moment and torque, i.e., $M_{ba} = M_{ta} = 0$, and therefore, $C = C_t = 0$. In simple turning and drilling operations, distinguished by formation of continuous chips, the characteristic values are $C = C_t = 0.1 – 0.2$. The variation of bending moment and torque is greater in intermittent cutting operations such as milling; for such operations $C = C_t = 0.3$–0.5.

The most important parameter in spindle design is the diameter of the front bearing journal. Typical values of this diameter are given in Table 5.3.[3]

Table 5.3   *Diameter (in mm) of front bearing journal[3]*

Power rating kW	Machine Tool		
	Lathe	Milling	Cylindrical Grinding
1.5–2.5	60–80	50–90	—
2.5–3.5	70–90	60–90	50–60
3.5–5.5	70–105	60–95	55–70
5.5–7.0	95–130	75–100	70–80
7.5–11.0	110–145	90–105	75–90
11.0–14.5	140–165	100–115	75–100
14.5–18.0	150–190	—	90–100
18.0–22.0	220	—	105
22.0–30.0	230	—	105

Some practical considerations which may be useful in spindle design are briefly discussed below.

1. **Additional Supports** The radial stiffness of a spindle can be improved by supporting it at more than two points. If an intermediate support is provided, the spindle constraints change from free supports to clamped supports, thereby increasing its stiffness. However, in multiple bearing spindles the support journals should be machined in one setting, as otherwise skewing and jamming of the spindle can occur due to large misalignment.

2. **Location of Bearings and Drive Elements** The bearings should be located as near as possible to the point of load application (spindle nose) to restrict bending deflection and buckling. The length of spindle between the spindle nose and the point where the drive element transmits torque is subjected to bending and torsion. It is, therefore, desirable that the drive element transmitting maximum torque to the spindle should be located as near as possible to the front bearing.

3. **Balancing** The satisfactory performance of high-speed spindles is possible only if the spindle unit (after mounting the gears, clutches, etc.) is dynamically balanced before assembly in the spindle head or headstock. For general-purpose machine tools the permissible value of disbalance is 25 g · cm at 2000 rpm.

5.5 ANTI-FRICTION BEARINGS

It was explained in Sec. 5.4.1 that the deflection of the spindle nose depends, besides other factors, upon the compliance of the front and rear spindle supports. The rotational accuracy, which is one of the basic functional requirement of a spindle is also greatly influenced by the choice of bearing. Owing to the diversity of operating conditions of spindles, anti-friction, hydrodynamic, hydrostatic, and lately, air-lubricated bearings are used as spindle supports in different machine tools. Irrespective of the type of bearing, the common requirements of spindle supports can be specified as

1. guiding accuracy,
2. ability to perform satisfactorily under various conditions of spindle operation,
3. high stiffness,
4. minimum heating, as this can lead to additional spindle deformation, and
5. vibration stability, which is governed mainly by the damping.

Anti-friction bearings are one of the most widely standardised elements in industry and are manufactured on a mass scale throughout the world. The distinguishing features of anti-friction bearings as compared to sliding bearings are:

1. Low frictional moments and heat generation.
2. Low starting resistance.
3. High load capacity per unit width of the bearing.
4. Easy maintenance and less consumption of lubricants.

On the basis of the shape of the rolling element, anti-friction bearings may be classified as ball and roller bearings. Ball bearings are less prone to heating, and therefore, permit larger rotational speeds. They are also cheaper than roller bearings and less sensitive to small alignment errors. However, roller bearings have higher load capacity.

A machine tool spindle experiences both axial and radial loads. These loads can be balanced either by bearings that take up radial and axial loads separately or by bearings that take up both. In this regard, it should be recalled that

1. cylindrical roller bearings can take up only radial load,
2. simple radial ball bearings are basically meant for taking up radial loads, but are generally able to support axial loads too,
3. angular contact ball bearings can take up radial loads as well as relatively large axial loads in one direction,
4. taper roller bearings can take up large radial and axial loads with equal ease,
5. ball thrust bearings are useful for supporting purely axial loads only, their maximum rotational speed is just about 60% of a radial ball bearing of equal size, and
6. cylindrical roller thrust bearings are not recommended for general use on account of sliding between rollers and races.

The number of possible combinations of various anti-friction bearings that can be employed in machine tool spindles to fulfil the basic function of supporting axial and radial loads is theoretically enormous. However, the viability of each combination must be assessed vis-a-vis the following parameters:

1. Radial stiffness of the spindle unit.
2. Axial stiffness of the spindle unit.
3. Radial run out of the spindle.
4. Axial run out of the spindle.
5. Heat generation.
6. Maximum permissible rotational speed, restricted by bearing wear and its heating.
7. Thermal deformation of the spindle.
8. Ease of manufacture and assembly of the spindle unit.

The relative performance and technological indices for eight combinations are given in Table 5.4.[4] It may be pointed that these combinations are typical of a majority of spindle units in small- and medium-size machine tools.

Based upon Table 5.4, some important operational features of different types of bearings can be summed up as under:

1. Use of taper roller bearings considerably increases both radial as well as axial run outs.
2. Use of only cylindrical roller bearings at the front support greatly enhances axial thermal deformation of the spindle nose.
3. Use of angular contact ball bearings at the front support results in low heat generation. This coupled with a fairly satisfactory axial stiffness permits high rotational speeds.

It is evident from Table 5.4 that no single combination of bearings is ideal for all performance indices. In each specific case, the selection of bearings is governed by the relative influence of the performance indices on the functional accuracy of the spindle unit. Table 5.5[5] contains this information for some of the major groups of machine tools.

The procedure for bearing selection is not described here and the reader should refer to a standard text on Machine Design or a manufacturer's catalogue for this purpose. However, some important features related to the performance of bearings are discussed as follows.

Table 5.4 *Relative comparison of performance and technological indices of spindle supports*

S. No.	Sketch	Radial stiffness	Axial stiffness	Radial run out	Axial run out	Heat general Front bearing	Common	Permissible rpm	Axial thermal deformation	Ease of manufacture and assembly
1.		1.0	1.0	1.0	1.0	1.0	1.0	1.0	1.0	A
2.		0.95	0.71	1.0	1.0	0.5	0.6	1.0	3.0	B
3.		1.0	3.0	1.0	1.0	1.2	1.15	0.75	1.0	A
4.		0.78	3.0	1.0	1.0	1.2	1.15	0.75	0.6	A
5.		1.0	2.5	1.0	1.0	0.5	0.75	0.8	3.0	B
6.		0.93	1.0	2.0	1.5	0.75	0.8	0.6	0.8	A
7.		1.05	1.0	2.0	1.5	1.4	1.4	0.6	0.8	A
8.		0.7	1.0	1.0	1.0	0.5	0.7	1.2	0.8	C

Notation: A—Very complicated   ▭ Cylindrical roller bearing   ▨ Angular contact ball bearing

       B—Complicated   ◈◈ Taper roller bearing   ◇◇ Ball thrust bearing

       C—Simple

Table 5.5 *Relative influence of performance indices on the functional accuracy of spindle units*

S. No.	Machine tool	Radial stiffness	Axial stiffness	Radial run out	Axial run out	Heat generation	Permissible rpm	Thermal deformation
1.	Lathes							
	(a) small-sized	I	I	D	D	D	D	I
	(b) medium-sized	D	I	D	D	I	I	I
	(c) single spindle automatic	D	I	D	D	I	I	D

Contd.

Table 5.5 *Contd.*

2.	Work head spindle of universal and internal grinding machine							
	(a) small-sized	D	U	D	D	U	U	U
	(b) medium-sized and heavy-duty	D	I	D	D	U	U	U
3.	Universal milling machine	D	D	D	D	I	I	D

Notation: D—of decisive importance; I—of average importance; U—of relatively minor importance

5.5.1 Preloading of Anti-friction Bearings

It has already been stated in Sec. 5.4 that the total deflection of spindle nose depends upon its own stiffness as well as the stiffness (compliance) of the spindle supports. The discussion which follows will reveal the positive role played by preloading of rolling elements in reducing the total deflection.

The variation of spindle deformation δ due to a radial force P is depicted in Fig. 5.12. If the bearing is assembled with a clearance, a reversal of the direction of the applied force results in an abrupt change of deformation (Fig. 5.12a). This is highly undesirable from the point of view of machining accuracy. Bearings assembled with interference are free of this shortcoming and are distinguished by a smooth δ-P curve (Fig 5.12b). It can be seen from Fig. 5.12 that the rate of deformation is initially high but later on decreases and at large loads becomes virtually constant. This is due to the fact that as the load increases, its distribution between the rolling members becomes more uniform. Since a larger number of rolling members support the increased load, the deformation reduces. The data of Table 5.6 depicts the influence of bearing play on the stiffness of the spindle unit.
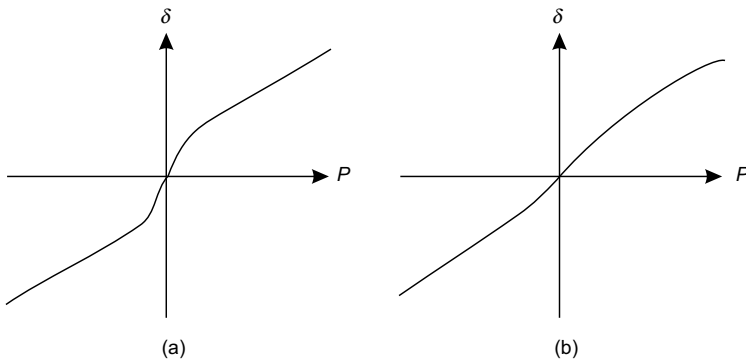

Fig. 5.12 *Effect of radial force on spindle deflection when (a) bearing is assembled with a clearance (b) bearing is assembled with an interference*

Table 5.6 *Effect of bearing play on spindle unit stiffness*[6]

S. No.	Play of front bearing, microns	Deflection of spindle nose due to		Total deflection of spindle nose, microns
		bending, microns	compliance of support, microns	
1.	15 (clearance)	14	16	30
2.	– 5 (interference)	13	6	19
3.	– 15 (interference)	11	5	16

It is evident from Table 5.6 that the assembly of a bearing with a small interference sharply reduces support deformation from 16 to 6 microns. The deflection due to bending of the spindle axis also reduces, though not so perceptibly. The reason for such behaviour is that as the interference increases, the end constraints change from a simply supported beam to those of a clamped beam. This is equivalent to providing an additional intermediate support, which predictably increases stiffness and results in less deflection of the spindle nose.

A glance at Table 5.6 revels that increase of interference from 5 to 15 microns barely yields a 1-micron reduction of support deflection from 6 to 5 microns. However, a large interference is accompanied by excessive heating and also reduces the bearing life on account of large contact deformation. Obviously, optimum interference is one which precludes clearance but does not result in excessive heating of the bearing. Interference in the assembly of rolling elements is achieved by preloading them.

Preloading of a bearing involves relative axial displacement of the inner and outer races by a small amount (Fig. 5.13). The methods of applying preloading in radial and angular contact ball bearings that are generally mounted in pairs are shown in Fig. 5.14. A constant preloading is achieved either by grinding off the faces of the inner races (Fig. 5.14a) or by inserting spacing rings of different widths between the inner and outer races (Fig. 5.14b). If the bearing rotates at high rpm, the initial preload has a tendency to weaken. In such cases, especially when bearings are small, the preloading can be applied by means of springs which ensure a constant preload that can be accurately adjusted (Fig. 5.14c). This method is adopted in precision bearings.
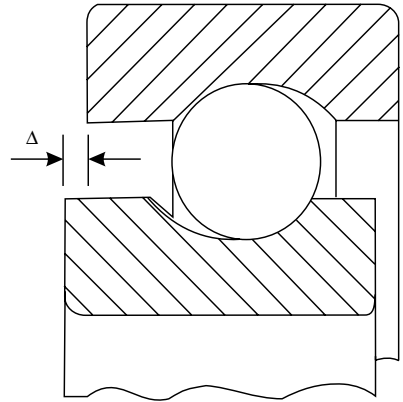

Fig. 5.13 *Schematic diagram depicting preloading by relative axial displacement of the bearing races*
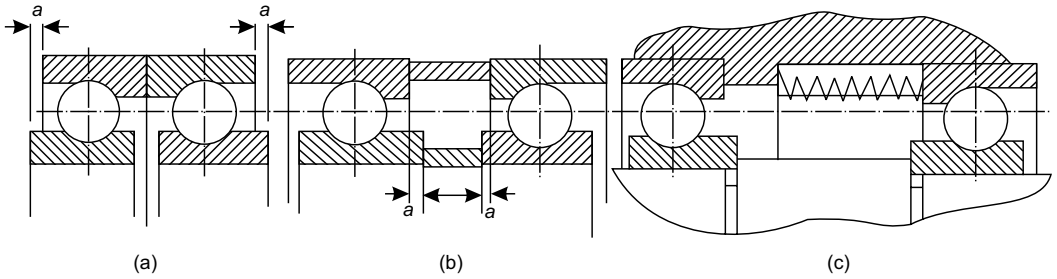
Fig. 5.14 *Methods of preloading ball bearings*

Cylindrical double roller bearings are generally mounted on tapered journals. The preloading is obtained through axial displacement of the inner ring with an adjusting nut (Fig. 5.15). The utility of this arrangement can be considerably improved by using a split nut. As the bearing wears, the preset value of preloading decreases. When this occurs, the split nut is removed, slightly ground and mounted again. The initial preloading is then reinstated by additional axial displacement of the adjusting nut by a distance equal to the ground layer removed from the split nut. However, this procedure should be discontinued after a few regrindings of the split nut, because when the bearing wear becomes large, the roller length is partially in contact with the worn surface of the race way and partially with the unworn surface. This results in excessive heat generation and non uniform rotation. Axial displacement of the bearing race by the threaded nut does not provide uniform contact of the face and can result in deformation of the spindle. The non-uniformity of face contact may be somewhat reduced by inserting a sleeve between the nut and bearing as shown in Fig. 5.15b. The spherical face of the sleeve should fit into an identical spherical seat on the nut face. Axial displacement of the bearing inner race is seriously impeded by large static friction between the inner race bore and the spindle. It requires an axial force of 2000–3000 kg to shift the race of a small bearing about 100 mm in diameter. Application of such large forces not only makes fine adjustment difficult but also fails to eliminate the misalignment (skewness) of the bearing race, resulting in poor rotational accuracy of the spindle. To reduce friction at the time of adjustment of bearing play, oil is force fed into the interface between the race bore and spindle.
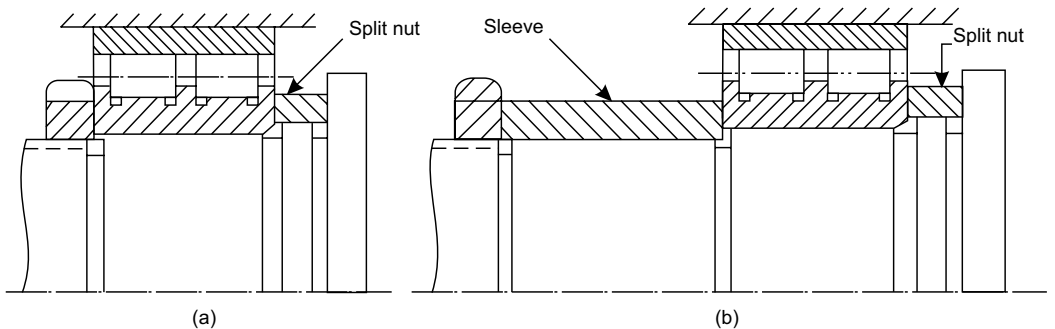

Fig. 5.15 *Methods of preloading cylindrical, double roller bearings*

The oil is supplied by an injector through a small oil hole in the spindle and an annular groove (Fig. 5.16). In this way, the required axial force for bearing adjustment can be reduced ten-fold. After completing the adjustment, the oil film is removed and the bearing inner race fits uniformly over the taper journal.
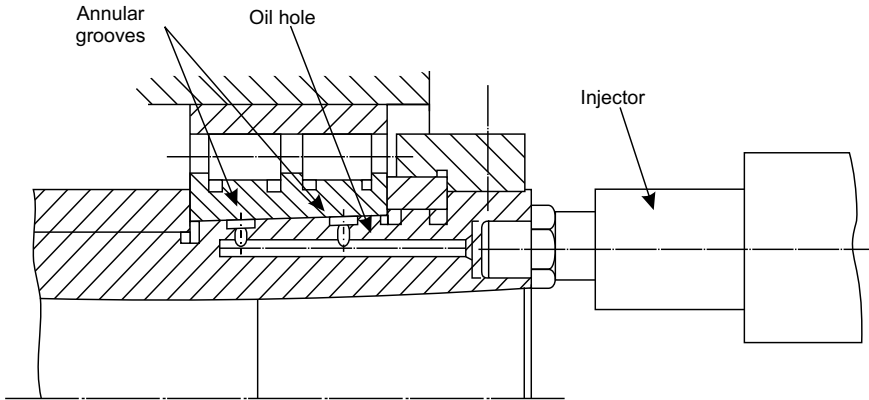

Fig. 5.16 *Schematic diagram describing the oiling arrangement to reduce friction at the bearing-spindle interface during bearing play adjustment*

Taper roller bearings are preloaded by the methods shown in Fig. 5.17. In the method shown in Fig. 5.17a, the inner and outer races are axially displaced with the help of nuts. This method is applied only in non-precision bearings because the axes of inner and outer races get skewed. In the Gamet bearing arrangement (Fig. 5.17b), the outer race is axially displaced by means of springs, whereas in the Timken bearing (Fig. 5.17c), this is achieved by supplying oil or air under controlled pressure.
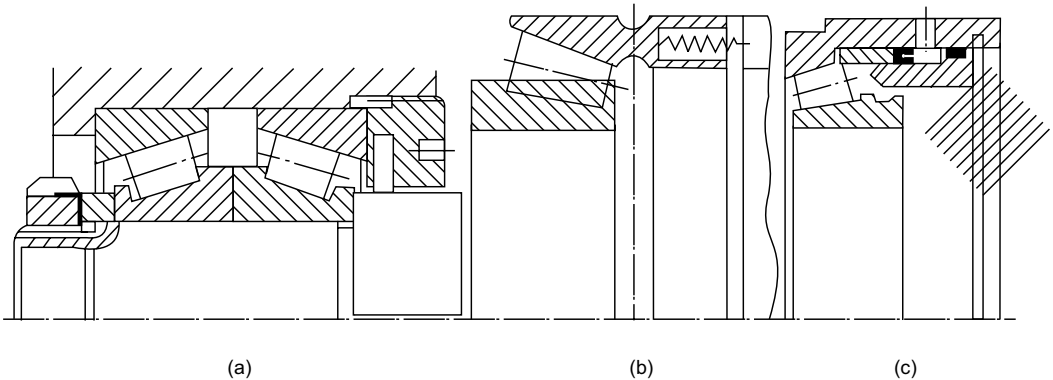

(a) (b) (c)

Fig. 5.17 *Methods of preloading taper roller bearings*

5.6 SLIDING BEARINGS

A major drawback of ball and roller bearings is their large radial dimension. This difficulty can be overcome by using needle roller bearings. However, wide application of needle bearings in machine tool spindles is restricted due to their large coefficient of friction, short service life and tendency to skew, particularly under an eccentric load. When there is a constraint of space, generally sliding bearings are preferred. Sliding bearings are used when

1. rotational speeds are so high that anti-friction bearings become uneconomical due to their short service life,
2. accuracy of spindle rotation is required to be very high, and
3. the bearings are subjected to shocks and vibrations; the inherent damping of sliding bearings is considerably greater than that of anti-friction bearings due to the presence of viscous fluid.

Sliding bearing is a general term that covers all bearings that do not use rollers or balls. These bearings operate under conditions of sliding friction between the bearing bore and spindle journal, which are separated by a lubricant film. Depending upon the film thickness, sliding bearings can be classified as

1. zero film bearings in which there is no lubricant,
2. thin film bearings in which the lubricant layer is not sufficiently thick to completely eliminate metal-to-metal contact; friction conditions at the interface of mating surfaces are of semi-liquid type and these bearings are known as sleeve bearings,
3. thick film bearings in which the mating surfaces are completely separated by the lubricant film. The excessive pressure required to sustain a permanent lubricant film may be hydrodynamic or hydrostatic in nature. Correspondingly, thick film bearings may be subclassified as hydrodynamic journal bearings or hydrostatic journal bearings.

The Hersi–Shtribek diagram shown in Fig. 5.18 depicts the variation of the coefficient of friction f as a function of the quantity

$$\lambda = \frac{\mu\omega}{p}$$

where μ = absolute viscosity of the lubricant
ω = angular velocity of rotation of the journal
p = average pressure per unit area of the supporting surface

Fig. 5.18   *Hersi-Shtribek diagram*

At very low rotational speed when $\lambda < \lambda_1$, the lubricant film is extremely thin—of the order of 0.1 microns—and the coefficient of friction practically does not change with λ. This region which lies to the left of point 1 of the Hersi-Shtribek diagram is distinguished by boundary lubrication in which zero-film bearings operate.

For higher values of λ lying between λ_1 and λ_2, the friction conditions are of semi-liquid type and the bearings operating under these conditions are known as thin film bearings. Beyond $\lambda > \lambda_2$, liquid friction conditions prevail and they represent the operating conditions of hydrodynamic bearings.
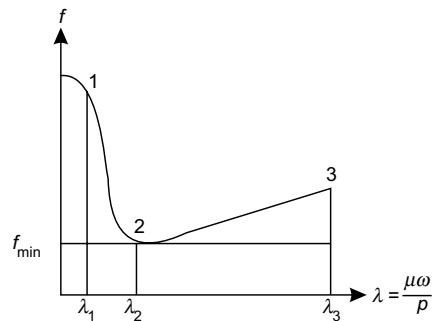
The sketch of a sliding journal bearing is shown in Fig. 5.19. Diameter d of the journal is always less than diameter D of the bearing. At zero rotational speed, the journal rests on the bearing and metal-to-metal contact takes place at point A (Fig. 5.19a). As the journal begins to rotate in the anti-clockwise direction, it tends to roll up the bearing surface due to the friction force and moves to a position B (Fig. 5.19b). The oil film now consists of two parts—a converging wedge above line BE and a diverging wedge below it. Owing to the hydrodynamic effect a positive pressure builds up in the converging wedge. This hydrodynamic force increases with increase of rotational speed and overcomes the frictional force. As a result, the point of contact moves to point C (Fig. 5.19c). As long as $\lambda < \lambda_2$, the metal-to-metal contact at point C persists. However, when the rotational speed is such that $\lambda > \lambda_2$, the hydrodynamic force becomes large enough to lift the journal and a continuous film is formed having minimum thickness at point D (Fig. 5.19d).
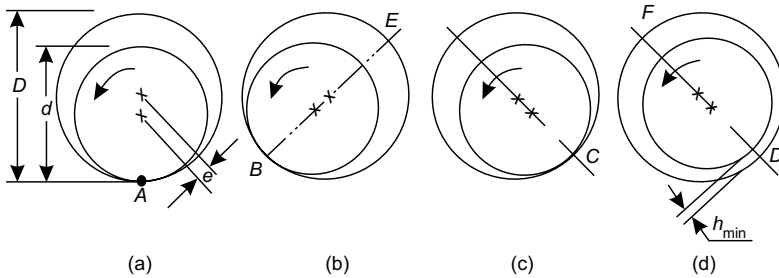
Fig. 5.19 *Schematic diagram describing the working principle of a sliding journal bearing*

Sliding journal bearings are classified as full (Fig. 5.20a) and partial (Fig. 5.20b and c). Partial journal bearings have less friction than a full journal bearing, but can be used only where the load always acts in one direction.

Fig. 5.20 *Types of sliding journal bearings: (a) Full (b) 120° partial (c) 120° fitted*

5.6.1 Sleeve Bearings

Sleeve bearings are designed for wear resistance. The design conditions are

$$p = \frac{P}{d \cdot l} \leq [p] \tag{5.41}$$

$$pv \leq [pv] \tag{5.42}$$

where p = bearing pressure
P = load on the journal
d = diameter of the journal
l = length of the bearing
v = peripheral speed
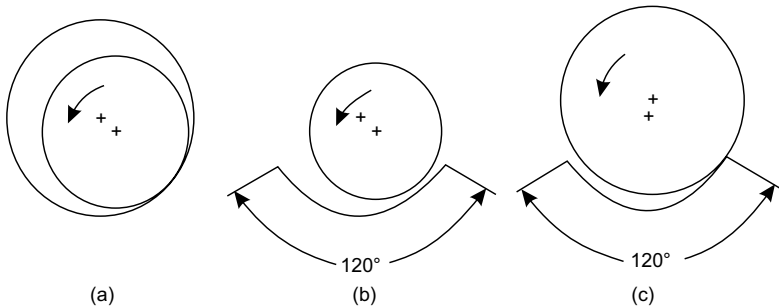$[p]$ = permissible value of bearing pressure
$[pv]$ = permissible value of the product of bearing pressure and peripheral speed

The permissible values of $[p]$ and $[pv]$ vary in a wide range depending upon factors such as bearing material, sliding velocity, cooling and lubrication conditions, etc. These are given for some important sliding bearing materials in Table 5.7.

Table 5.7   *Permissible values of [p] and [pv] for some bearing materials*

S. No.	Material	v, m/s	[p], kgf/cm²	[pv] kgf, m/cm² · s
1.	Grey iron	0.5	40	
		1.0	20	
		2.0	1.0	
2.	Anti-friction cast iron	0.2	90	18
		2.0	0.5	1.0
3.	Modified anti-friction cast iron	1.0	120	120
		5.0	5.0	25
4.	Bronze	3	50	100
5.	Aluminium bronze	4	150	150
6.	Tin bronze	10	150	150
7.	Graphite bronze (20–25% porosity)	0.2	60	
		0.4	10	
8.	White metal	12	250	300
9.	Aluminium alloy	12	250	300
10.	Zinc alloy	10	120	120

The selection of the sliding bearing material is based upon the following considerations:

1. High wear resistance.
2. High fatigue strength.

3. High compressive strength.
4. High thermal conductivity.
5. High conformability to accommodate spindle deformations and reduce edge pressures.
6. High corrosion resistance.
7. Low modulus of elasticity.

Typical values of p and v that occur in machine tool spindle units and the recommended sliding bearing materials are given in Table 5.8.

A sliding bearing made from anti-friction cast iron has poor conformability, therefore, the spindle should have high stiffness to avoid large pressures. Copper alloy compositions are used in the form of bimetallic sleeves. A layer of approximately 1.0 mm thickness is deposited on a steel or cast iron sleeve by the centrifugal casting method. Porous graphite bronze bearings are employed at low sliding speeds under conditions of variable loading. Aluminium alloy is employed as a replacement for white metal and zinc alloy for babbits.

Table 5.8 *Recommended compositions of sliding bearing materials*

S. No.	v, m/s	p, kgf/m² <	pv, kgf, m/cm² · s <	Recommended material
1.	2	10	20	Anti-friction cast iron
2.	2.5	8–16	20–40	Zinc alloy (84.5–86.5% Zn, 9–11% Al, 4.5–5.5% Cu)
3.	5	8–12	40–60	Aluminium alloy (88–91% Al, 7.5–9.5% Cu, 1.5–2.5% Si)
4. (a)	5	12–16	60–80	Bronze (86% Cu, 6% Sn, 6% Zn, 3% Pb)
(b)	5	12–16	60–80	Aluminium bronze (87% Cu, 9% Al, 4% Fe)
5.	10	8–10	80–100	White metal (68.5–71.5% Cu, 27.5–31.5% Pb)
6.	10	10–12	100–120	Tin bronze (89.5% Cu, 10% Sn, 0.5%, Pb)

5.6.2 Hydrodynamic Journal Bearings

As already stated in Sec. 5.6.1, a sleeve bearing begins to operate as a hydrodynamic bearing when $\lambda > \lambda_2$. The angular velocity at which the transformation from semi-liquid friction to liquid friction occurs is given by the expression,

$$\omega_2 = \frac{p \cdot \psi^2}{\mu \cdot S_0}, \text{ s}^{-1} \tag{5.43}$$

where p = average bearing pressure, kgf/m^2

$\psi = \dfrac{D - d}{d}$ = relative diameteral clearance

μ = absolute viscosity of lubricant, kgf · s/m^2

S_0 = critical value of Sommerfeld number

Obviously, when $\omega > \omega_2$, the conditions are those of liquid friction, whereas when $\omega < \omega_2$, the conditions are of semi-liquid type. The values of S_0 are given in Table 5.9.

The theory of hydrodynamic lubrication has been successfully developed to yield design expressions for idealized journal bearings or infinite bearings. The expressions for an idealised bearing are derived on the basis of the assumption that there is no flow in the axial direction, i.e., there is no end leakage. The bearing parameters that must be determined are discussed below.

1. **Length to Diameter (l/d) Ratio**   The optimum value of l/d ratio that is often recommended is l. A larger l/d ratio can be taken when the rigidity and alignment conditions are favourable and cooling of the system is

Table 5.9   *Critical values of the Sommerfeld number S_0*

l/d	Journal diameter d in mm								
	30	40	50	60	70	80	100	150	200
$\psi = 0.001$									
0.6	0.28	0.35	0.42	0.53	0.65	0.8	1.0	2.0	3.0
0.8	0.44	0.54	0.64	0.80	0.95	1.2	1.5	2.7	4.0
1.0	0.58	0.72	0.85	1.0	1.2	1.5	1.9	3.3	4.5
1.2	0.70	0.80	1.0	1.2	1.4	1.7	2.2	3.7	5.0
$\psi = 0.002$									
0.6	0.42	0.53	0.65	0.8	1.0	1.4	2.0	3.0	5.0
0.8	0.64	0.80	0.95	1.2	1.5	1.9	2.7	4.0	6.0
1.0	0.85	1.0	1.2	1.5	1.9	2.4	3.3	4.5	7.0
1.2	1.0	1.2	1.2	1.7	2.2	2.6	3.7	5.0	8.0
$\psi = 0.003$									
0.6	0.65	0.8	1.0	1.4	2.0	3.0	4.0	5.0	6.0
0.8	0.96	1.2	1.5	1.9	2.7	4.0	5.0	6.0	8.0
1.0	1.2	1.5	1.9	2.4	3.3	4.5	6.0	7.0	9.0
1.2	1.4	1.7	2.2	2.6	3.7	5.0	6.5	8.0	10.0

not a problem. A value of l/d ratio less than 1 is selected when the shaft deflection is significant and greater flow of lubricant is required to improve cooling.

While selecting the l/d ratio, it should generally be borne in mind that a larger l/d ratio provides for a greater film force, but at the same time also reduces heat dissipation thus leading to heating of the bearing. Also, a bearing with a large l/d ratio is more susceptible to the metal-to-metal contact between the bearing and journal surfaces.

2. **Bearing Clearance**   The diametral clearance significantly affects the performance of a hydrodynamic bearing. The minimum clearance should be such that it ensures a continuous lubricant film between the journal and bearing. This clearance, also known as critical clearance, can be found from the expression,

$$h_{cr} = R_{zb} + R_{zj} + y_0 = \frac{D - d}{2} = \frac{\psi d}{2} \tag{5.44}$$

where R_{zb} = height of micro irregularities on the bearing surface
R_{zj} = height of micro irregularities on the journal surface
y_0 = deflection of the supported length of the journal

In design practise, the following approximate expression, which provides for a certain margin of safety, can be used.

$$h_{cr} = 2(R_{zb} + R_{zj}) \tag{5.45}$$

An increase of clearance reduces the load capacity of the bearing, but at the same time increases the flow rate of the lubricant and hence brings down the operating temperature. The following values of ψ can be used as a guide for preliminary selection for different bearing materials (Table 5.10).

In general, the greater the l/d ratio and ω, and the lower the pressure p, the higher should be the bearing clearance. The following two empirical relationships may be used for approximate calculation of the ψ value:

Table 5.10   *Recommended value of ψ different bearing materials*

Bearing materials	$\psi = (D - d) / d$
Tin base babbit	0.0005
Cadmium silver	0.0008
Copper-lead	0.001
Silver-lead-indium	0.001
Aluminium	0.001

$$\psi = 0.001 + \frac{0.0508}{d} \tag{5.45}$$

$$y = 0.8 \times 10^{-3} v^{0.25} \tag{5.46}$$

where v is the peripheral speed in m/s

d is the journal diameter in mm

The recommended values of diametral clearance $D - d$ for various machine tools are given below:

High precision machines	0.004–0.010 mm
Grinding machines	0.010–0.015 mm
Normal accuracy lathes	0.015–0.025 mm
Automatic and production lathes	0.020–0.025 mm
Normal accuracy milling and drilling machines	0.02–0.03 mm

3. **Viscosity of Lubricant**   After having found ψ, the required viscosity of the lubricant that ensures hydrodynamic lubrication can be determined from the expression,

$$\mu \geq \frac{p\psi^2}{\omega S_0} \text{ kgf} \cdot \text{s/m}^2 \tag{5.47}$$

where S_0 represents the critical Sommerfeld number. It is not desirable to select a lubricant with a viscosity much greater than the minimum essential, because this leads to increase of frictional losses in the bearing.

4. **Load Capacity and Load Coefficient**   The load capacity of a hydrodynamic bearing is given by the expression,

$$P = \frac{\mu\omega}{\psi^2} \cdot l \cdot d \cdot C_L \tag{5.48}$$

here l and d are in m, and C_L represents the load coefficient. This coefficient depends upon the l/d ratio and the eccentricity ratio ε, which is defined as

$$\varepsilon = \frac{e}{c} \tag{5.49}$$

$$c = \frac{D - d}{2} = \frac{d\psi}{2}$$

is known as the *radial clearance*.

Load coefficient C_L is related to the Sommerfeld number S by the expression $C_L = 1/2\pi S$. For different values of d/l and ε, the value of load coefficient C_L can be determined from Table 5.11.

Table 5.11 *Load coefficient C_L for hydrodynamic journal bearings*

l/d	ε						
	0.4	*0.5*	*0.6*	*0.7*	*0.8*	*0.9*	*0.975*
360° Full bearing							
0.25	0.0559	0.0887	0.1472	0.2697	0.5981	2.08	15.758
0.5	0.2023	0.3121	0.4972	0.8563	1.716	4.935	26.134
0.75	0.3905	0.5969	0.911	1.4846	2.7435	6.9167	—
1.00	0.6121	0.8896	1.315	2.0394	3.6171	8.272	33.576
1.25	0.8161	1.1617	1.6753	2.5182	4.1882	9.1468	—
1.5	1.0009	1.4011	1.9648	2.8754	4.6400	9.830	—
180° Partial bearing							
0.5	0.209	0.317	0.655	0.819	1.572	4.261	25.62
0.7	0.361	0.538	0.816	1.312	2.399	6.029	31.88
1.00	0.589	0.853	1.263	1.929	3.372	7.772	37.00
1.20	0.723	1.033	1.489	2.247	3.787	8.533	39.04
1.5	0.891	1.248	1.763	2.60	4.266	9.304	41.07
120° Partial bearing							
0.5	0.188	0.261	0.462	0.826	1.676	4.717	29.33
0.70	0.299	0.441	0.709	1.221	2.365	6.213	34.30
1.00	0.436	0.633	0.992	1.644	3.042	7.508	38.08
1.20	0.506	0.722	1.126	1.838	3.335	8.075	39.58
1.5	0.583	0.831	1.271	2.041	3.667	8.618	41.06

After having determined the l/d ratio, ψ and μ, the designer will be faced with one of the two design problems which are discussed as follows.

Design Problem 1   The load on the bearing is known and it is required to check whether the bearing having the l/d, ψ and μ values as found above, will perform satisfactorily.

In this case, the load coefficient C_L is determined from Eq. (5.48). Then for the known l/d ratio, the eccentricity ratio ε is determined from Table 5.11. Now, knowing ε and radial clearance c, the minimum film thickness is determined from the expression,

$$h_{min} = c(1 - \varepsilon) \tag{5.50}$$

If $h_{min} > h_{cr}$, the bearing operates under liquid-friction conditions and the design may be accepted. If, however, $h_{min} < h_{cr}$, then corrective measures must be taken. These may be

1. reducing h_{cr} by improving the surface finish of the bearing and journal surfaces,
2. increasing h_{min} either by increasing c or by increasing the l/d ratio as this yields a smaller value of ε.

Design Problem 2   The minimum film thickness is known and it is required to check whether the bearing having l/d, ψ and μ values as found above will be able to take the operating load.

The recommended values of h_{min} for different conditions are given in Table 5.12. These values satisfy the condition $h_{min} > h_{cr}$.

Table 5.12   *Recommended value of h_{min} for different conditions*

S. No.	Operating condition	h_{min}, mm
1.	In order to pass dirt particles and prevent scoring	0.0026
2.	Finely bored bronze bearing	0.0026
3.	Fine finished bronze bearings used in automobile and aircraft engines	0.0026
4.	Babbit bearings running at high speeds	0.02
5.	General recommendation	0.0015–0.0002 mm per mm of the bearing diameter

For the known value of c and the selected value of h_{min}, the eccentricity ratio ε is determined from Eq. (5.50). Next, for the particular values of l/d ratio and ε, the load coefficient C_L is found from Table 5.11. Knowing the load coefficient, the bearing capacity is determined from Eq. (5.48). If it is found that the bearing capacity is less than the load acting on it, the former must be improved by taking appropriate corrective measures, which include

1. reduction of ψ, i.e., reduction of clearance by improving the surface finish of journal and bearing surfaces. This enables to reduce the minimum film thickness, thus providing for a greater value of ε and hence a higher value of load coefficient C_L,
2. increase of μ, i.e., application of a more viscous lubricant,
3. increase of bearing dimensions. The diameter of the journal is generally fixed from other design considerations, and therefore, only l may be increased, thus providing a greater l/d ratio. The l/d ratio indirectly contributes to a further increase in the bearing capacity as the load coefficient increases with the l/d ratio.

Check for Thermal Equilibrium   The rotation of a journal in a hydrodynamic bearing is resisted by the lubricant. The viscous friction offered by the lubricant results in a frictional force which must be overcome by the rotating journal. This leads to heat generation in the lubricant film. The essential design check for hydrodynamic bearings is

$$t_b \leq [t_b] \qquad (5.51)$$

where t_b = temperature of the bearing

$[t_b]$ = permissible value of bearing temperature; generally $[t_b] = 60–75°C$

The heat is dissipated through the housing, bearing body and journal. If the thermal equilibrium between heat generated and heat dissipated is established such that the bearing temperature is less than the permissible, then the design is accepted. However, if the reverse takes place, then either the design parameters should be modified or forced circulation of the lubricant should be introduced. In the latter case, it is necessary to determine the flow rate of the lubricant that ensures that Eq. (5.51) is not violated.

The heat generated can be determined from the expression,

$$\left. \begin{array}{l} W = f \cdot P \cdot \dfrac{\omega d}{2}\,\text{kgf} \cdot \text{m/s} \\[2mm] = \dfrac{3600}{427} \cdot \dfrac{f \cdot P \cdot \omega d}{2}\,\text{k cal/h} \end{array} \right\} \tag{5.52}$$

where P = load on the bearing

ω = rotational speed of the journal

For an unloaded bearing, the coefficient of friction can be calculated from the relationship,

$$f = \frac{\pi}{\psi}\,\frac{\mu\omega}{p} \tag{5.53}$$

The coefficient of friction of a loaded bearing is higher and can be found from the following formulae:

$$f = \frac{\pi}{\psi}\,\frac{\mu\omega}{p} + 0.55\,\psi\eta \tag{5.54}$$

for short bearing having $\dfrac{l}{d} < 1$, $\eta = \left(\dfrac{d}{l}\right)^{1.5}$

for bearings having $\dfrac{l}{d} > 1$, $\eta = 1$

The heat dissipation through the body and shaft is assumed to be proportional to the free surface area of the bearing assembly. It is given by the expression,

$$W_1 = kA(t_b - t_a)\text{kcal/h} \tag{5.55}$$

where k = heat transfer coefficient, kcal/m$^2 \cdot$ h $\cdot$ °C

A = free surface area of the bearing assembly, m^2

t_a = ambient temperature, °C

t_b = bearing temperature, °C

The heat-transfer coefficient k can be found from the following expression:

$$k = 6 + 10\sqrt{v} \tag{5.56}$$

where v = relative velocity of air flow surrounding the bearing assembly in m/s; it depends upon the rotational speed of the journal and has a minimum value of 1 m/s

Generally, k, lies between 25–35 kcal/m$^2 \cdot$ h $\cdot$ °C

The free surface area of the bearing assembly depends upon the design and size of the bearing. On an average, it may be taken equal to $25d^2$ or $20dl$. However, for very simple assemblies, it may reduce to $12dl$, whereas for bearings mounted in high housings it may go up to $40dl$. An additional area of $(5–8)d^2$ per journal should be added to the above to account for heat dissipation through the journal. The lower value of $5d^2$ is recommended for small bearings ($d < 100$ mm), while the higher value of $8d^2$ is for large bearings ($d > 100$ mm).

For thermal equilibrium, Eqs (5.52) and (5.55) are equated and the bearing temperature t_b is calculated. If t_b is found to be less than the permissible value, there is no need for forced circulation of the lubricant. However, if t_b exceeds the permissible value, forced lubricant circulation is essential to carry away the extra heat. Heat dissipation through the lubricant flowing in a hydrodynamic bearing is given by the following expression:

$$W_2 = 60CQ\gamma(t_0 - t_i), \text{kcal/h} \tag{5.57}$$

where C = specific heat of the lubricant, kcal/kg $\cdot$ °C

Q = flow rate of the lubricant, l/min

γ = density of the lubricant, g/cm^3

t_o = oil temperature after circulation through the bearing, °C

t_i = oil temperature when it enters the bearing, °C

The required flow rate which ensures that the bearing temperature remains less than the permissible value is calculated from the following thermal equilibrium equation after substituting $t_b' = [t_b]$ the expression for W_1.

$$W = W_1 + W_2 \tag{5.58}$$

Before supplying to the bearing, the lubricant must be thoroughly cleaned by fine filters to catch hard particles more than 2–3 microns in size. The oil is supplied at a pressure of 0.1–0.2 kgf/cm^2 which is enough to provide filling of the oil bath and preclude suction of air into the working zone of the bearing.

Finite Bearing   Design considerations have been discussed till now with reference to an idealized hydrodynamic bearing which presumes that there is no lubricant flow in the axial direction and hence no end leakage. In an actual bearing, there is always some leakage of the lubricant at the ends. This reduces the load capacity of the bearing. Also, in order to maintain a continuous lubricant film, a sufficient quantity of the lubricant must be supplied to compensate the leakage loss. An important question that arises in this context is where to introduce the lubricant. In Fig. 5.19d, the wedge below line *DF* is diverging, and therefore, develops zero, or even, negative pressure. The negative pressure can cause a rupture of the lubricant film, thus violating the conditions of fluid friction between the journal and bearing. To avoid rupture of the continuous film around the journal, the lubricant must be introduced into the bearing through an oil hole or oil groove in this region.

The load capacity of a finite journal bearing can be obtained by multiplying the load capacity of an infinite bearing of identical parameters with the load leakage coefficient n_p. This coefficient depends upon the l/d

ratio and ε. It is plotted in Fig. 5.21 as a function of $\pi d/l$ for different values of ε. Also plotted on the same diagram are the curves for friction leakage coefficient (n_F). The correction factor for coefficient of friction f can be determined as

$$n_f = \frac{n_p}{n_F} \qquad (5.59)$$

Thus the load capacity of a finite hydrodynamic journal bearing can be expressed as

$$P = \frac{\mu\omega}{\psi^2} l \cdot d \cdot C_L \cdot n_P \ \text{kgf} \qquad (5.60)$$

While checking the thermal equilibrium of a finite bearing to determine the bearing temperature, heat generated in the lubricant can be determined as follows:

$$W = n_f \cdot f \cdot P \cdot \frac{\omega d}{2} \qquad (5.61)$$

Though the curves for load leakage coefficient n_P and friction leakage coefficient n_F have been presented in Fig. 5.21 only for a 120° partial bearing, these values can be used with satisfactory approximation for journal bearings having different angles.
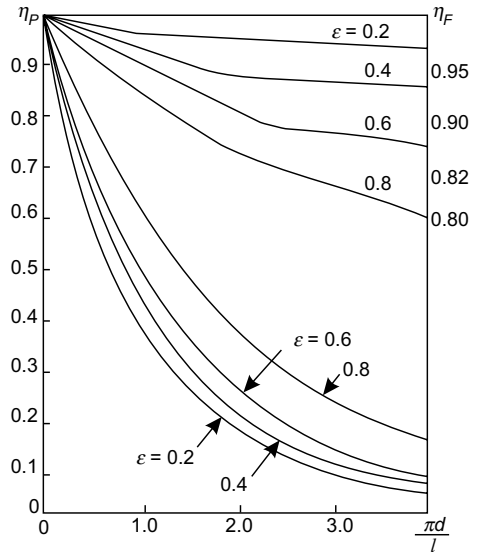
Fig. 5.21 *Leakage factors for load and friction force in 120° partial journal bearings*

Multiple-wedge Bearings The hydrodynamic journal bearing discussed till now has only one converging wedge and is called single-wedge bearing. One of the major shortcomings of these bearings is that the position of the journal inside the bearing varies with the load and rotational speed. This positional change leads to unstable running of the journal, which is impermissible in spindles of high accuracy and precision machine tools. These requirements are met in bearings having several converging wedges which uniformly surround the journal on all sides and ensure that during rotation the position of the journal changes very little or not at all. These bearings are known as *multiple-wedge bearings*. Figure 5.22 shows a self-adjusting tilting-pad journal bearing in which the wedges are formed due to tilt of the pads. These bearings generally have three to eight wedges.

The recommended values and expressions for calculating the design parameters of multiple-wedge bearings are discussed below.[7]

Fig. 5.22 *Schematic diagram of a multiple-wedge bearing*

1. **Ratio of pad length l to journal diameter d**

   $l = 0.75d$ for grinding machines

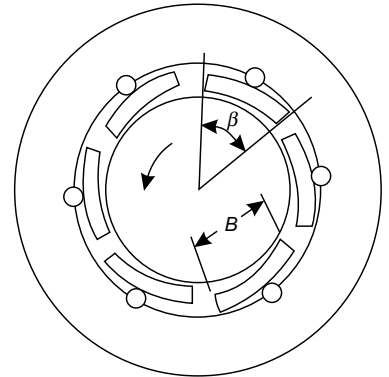 $l = (0.85\text{–}0.9)$ for high precision lathes and boring machines

2. **Pad width B**   The pad width should be such that it subtends an angle of $\beta = 50\text{--}60°$ at the centre. It should generally satisfy the condition

$$B = (0.6 - 0.8\ )l$$

3. **Radial clearance c**   The minimum clearance between the pad and journal depends upon their surface finish. If the surfaces are finish ground and honed ($R_z = 0.8\text{--}1.6$ microns), then

$$\text{For } d = 30\text{--}50 \text{ mm,} \qquad c = 3\text{--}5 \text{ micron}$$
$$\text{For } d = 50\text{--}100 \text{ mm,} \qquad c = 5\text{--}10 \text{ micron}$$
$$\text{For } d = 100 \text{ mm,} \qquad c = 10\text{--}15 \text{ micron}$$

4. **Viscosity of lubricant**   In multiple-wedge journal bearings, low viscosity oils are used. The recommended kinematic viscosity of the oil is 4–8 cS at 50°C, which corresponds to an absolute viscosity of 4–8 cP. It is not recommended to obtain the desired viscosity by diluting thick oil with a paraffin oil such as kerosene because the resultant mixture has poor lubricating properties and gradually becomes more viscous due to evaporation of the paraffin oil.

5. **Bearing capacity**   The bearing capacity is calculated approximately, assuming each wedge to be a slider bearing. The load capacity per wedge of an unloaded bearing is given by the expression,

$$P_0 = 10^{-2} \frac{\mu n \, dB^2 \cdot l}{(2c)^2} \cdot C_{L2}, \text{ kgf} \tag{5.62}$$

where μ = absolute viscosity of the lubricant, cP

$\qquad n$ = rpm of the journal

$$C_{L2} = \frac{1.25}{1 + (B/l)^2} = \text{load coefficient}$$

$\qquad d, B, l$ are in cm; c is in microns

It is evident from Eq. (5.72) that considerable hydrodynamic force is developed in each wedge even if there is no load on the bearing. These forces balance each other and tend to retain the rotating journal concentric with the bearing bore. When a load acts on the spindle, it gets displaced to a position defined by eccentricity e. External load P and eccentricity e are related through the expression,

$$P = P_0 \left[\frac{1}{(1 - 0.5\varepsilon)^2} - \frac{1}{(1 + \varepsilon)^2} \right] \tag{5.63}$$

where $\varepsilon = e/c$ is the eccentricity ratio.

Equations (5.62) and (5.63) can be used for solving the two general design problems which have been earlier discussed with reference to single-wedge bearings.

As a rule, multiple-wedge hydrodynamic journal bearings are provided with forced circulation of the lubricant. Assuming that heat dissipation through the bearing assembly and housing is negligible as compared to the heat carried away by the circulating lubricant, the increase in temperature of the lubricant can be calculated from the expression,

$$\Delta t = \frac{860 N_F}{C \gamma Q} \text{ °C} \tag{5.64}$$

where C = specific heat of the lubricant, kcal/kg · °C.

   γ = density of the lubricant, g/cm^3

   Q = flow rate of the lubricant, 1/h

   N_F = power loss due to friction, kW

The frictional power loss can be found from the following relationship:

$$N_F = 7.5 \times 10^{-10} \, \mu \, n^2 d^3 z \text{ kW} \tag{5.65}$$

where μ = absolute viscosity of the lubricant, cP

   z = number of wedges

   d = diameter of the journal, cm

Equations (5.64) and (5.65) enable us to determine the required flow rate which ensures that the bearing temperature remains less than its specified permissible value.

5.6.3   Hydrostatic Journal Bearings

Hydrodynamic journal bearings do not have sufficient stiffness to produce a circular profile with accuracy of the order of 0.1–0.2 microns. Besides, the stiffness of hydrodynamic bearings changes with lubricant viscosity, temperature and rotational speed of the journal. These shortcomings are absent in hydrostatic journal bearings. The basic features and principle of operation of hydrostatic journal bearings are essentially similar to those of hydrostatic pad bearings discussed in Sec. 4.4.1. Hydrostatic journal bearings may be single-pad (Fig. 5.23a), multiple-pad (Fig. 5.23b) and multiple-recess (Fig. 5.23c) type.
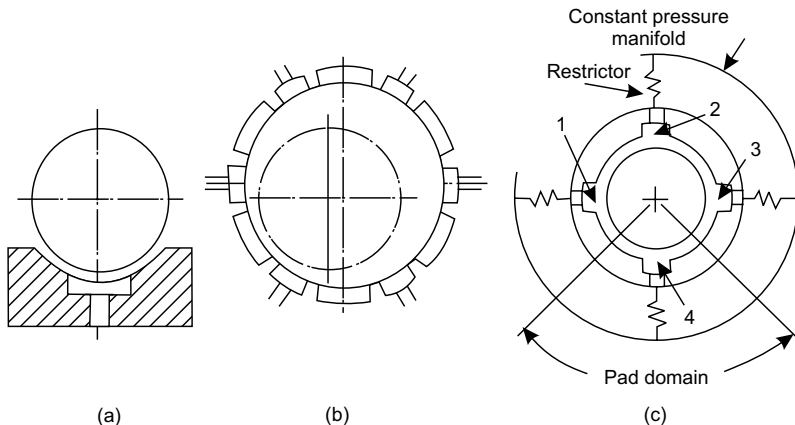

Fig. 5.23   *Types of hydrostatic bearings: (a) Single-pad (b) Multiple-pad (c) Multiple-recess*

The single-pad journal bearing has less than 180° included angle and normally supports only unidirectional load akin to partial hydrodynamic bearings. Multiple-pad bearings are employed when the load to be

supported is not unidirectional and varies as much as $\pm 180°$, e.g., an oscillating load, a reversing load, etc. In multiple-pad bearings, the number and location of pads are dictated by the angular variation of the applied radial load. For instance, a single-pad having the included angle $> 60°$ is adequate to support a purely unidirectional load. Two pads at an angle of $120°$ can be employed when the load varies within a maximum of $80°$. If a purely reversing radial load acts on the journal, a two-pad bearing having pads $180°$ apart can be used. For the general case in which load variation can assume any arbitrary value, we can use multiple-pad bearings having three or more pads distributed round the journal. Single-pad and multiple-pad bearings are rarely used in machine tool spindles due to the fact that there is considerable variation in direction as well as the magnitude of the cutting force depending upon cutting conditions, type of machining operation and other factors.

Multiple-recess bearings are akin to full (360°) hydrodynamic journal bearings and they can support all types of radial loads, including reversing and rotating loads. In common practise, the term hydrostatic journal bearing is understood to stand for a multiple-recess journal bearing and, therefore, the simpler term will be used in all subsequent discussion. The main difference between a multiple-pad and multiple-recess bearing is the absence of pressure-relieving grooves between the pads in the latter. Due to this, the pressure between the recesses does not go down to zero as in multiple-pad bearings, with the result that less flow through each recess is required to attain a similar preload film force when the journal and bearing are concentric.

Figure 5.23c shows a full hydrostatic journal bearing having four oil pockets located at $90°$ to each other. The lubricant is supplied to each pocket through an individual restrictor. When there is no load on the journal, the latter occupies a concentric position. The clearances between the journal and bearing are equal and so are the pressures in the recesses. Now assume that an external load acts on the journal, moving it towards recess 4 and away from recess 2. The film thickness in the clearance between recess 4 and the journal decreases, thereby resulting in reduced flow of the lubricant through this clearance. If a capillary or orifice type restrictor is being employed, the reduction of flow through the pocket will be accompanied by a decrease in pressure drop Δp across the restrictor, resulting in higher recess pressure which tends to restore the journal to the initial concentric position. If the restrictor used is a constant-flow type, then as the film thickness decreases, the pocket pressure must be increased to maintain a constant rate of flow.

The basic expressions for load capacity and flow in a hydrostatic journal bearing with uniform clearance are similar to the corresponding Eqs (4.44), (4.45) and (4.46) for a flat pad bearing. The load capacity of a hydrostatic bearing pad when the journal is in a concentric position is known as pad preload force and it is given by the expression,

$$P_{pr} = C_L \cdot A \cdot p_0 \qquad (5.66)$$

where C_L = load coefficient of the pad
  A = pad area, m^2
  p_0 = pocket pressure, kgf/m^2

Flow through the pocket is

$$Q_{pr} = \frac{p_0 h^3}{\mu C'_F} m^3/s \qquad (5.67)$$

where h = film thickness, m
  μ = absolute viscosity of the lubricant, $kgf \cdot s/m^2$

$\dfrac{1}{C'_F}$ = flow coefficient of the pad

The load and flow coefficients depend upon the shape and dimensions of the pocket and pad. For a cast bronze cylindrical pad with a circular pocket, these coefficients may be obtained from Fig. 5.24.[8] Rectangular pads with rectangular pockets are of two types:

1. Pads with equal sill lengths.
2. Pads with sill lengths in axial and circumferential directions proportional to the pad length in the same directions.

The pad coefficients for cast bronze cylindrical pads of the above two types are given in Figs 5.25–5.28.

Strictly speaking, the multiple-recess hydrostatic journal bearings do not have individual pads. Pad coefficients are obtained for the domain of each recess which extends halfway to each adjoining recess in the circumferential direction. Thus, in Eq. (5.66), A is taken as the area of the domain of each pocket. When a radial load acts on the journal, the non-symmetrical pressure distribution influences the effective values of pad coefficients. It is extremely difficult to determine the pad coefficients for non-uniform clearance. Therefore, the practical hydrostatic journal bearing design is rather conservative and is based on the pad coefficients given in Figs 5.24–5.28 at supply pressure,
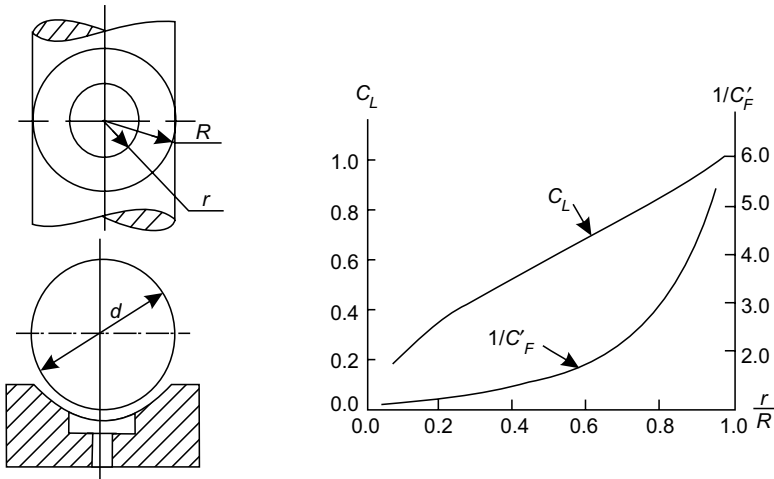
$$p_p = 2p_0 \tag{5.68}$$

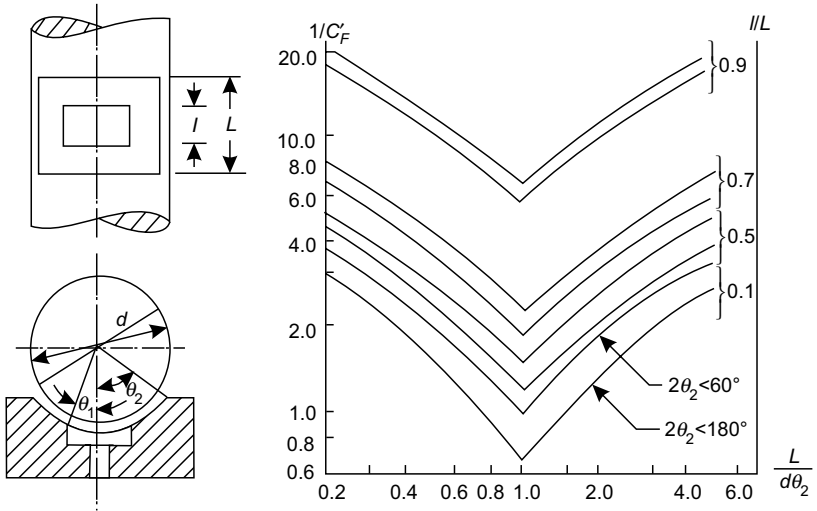**Fig. 5.24** *Load and flow coefficients for a cylindrical pad with circular pocket*

Fig. 5.25 *Flow coefficient for a cylindrical pad with rectangular pocket having equal sill lengths (L − l = θ₂ − θ₁)*
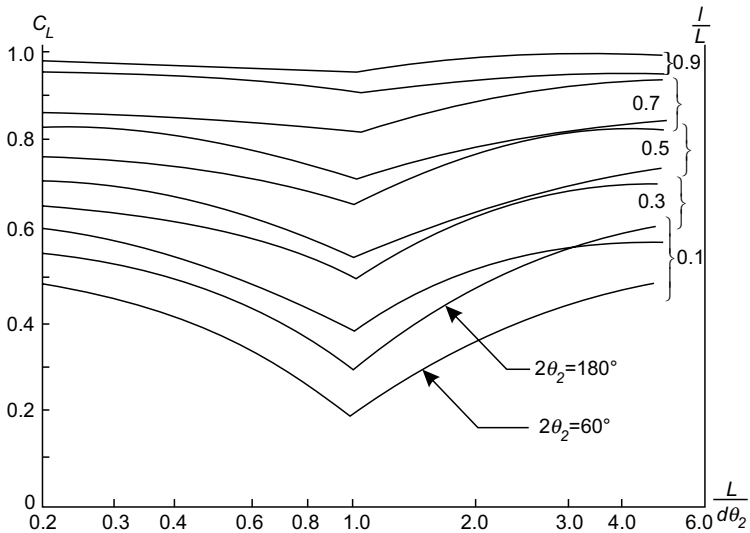

Fig. 5.26 *Load coefficient for a cylindrical pad with rectangular pocket having equal sill area*
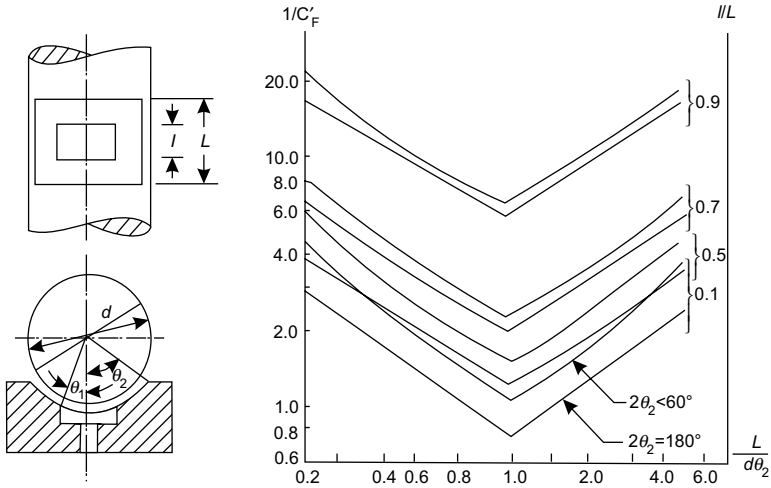
Fig. 5.27 *Flow coefficient for a cylindrical pad with rectangular pocket having equally proportional sill lengths* $(l/L = \theta_1/\theta_2)$
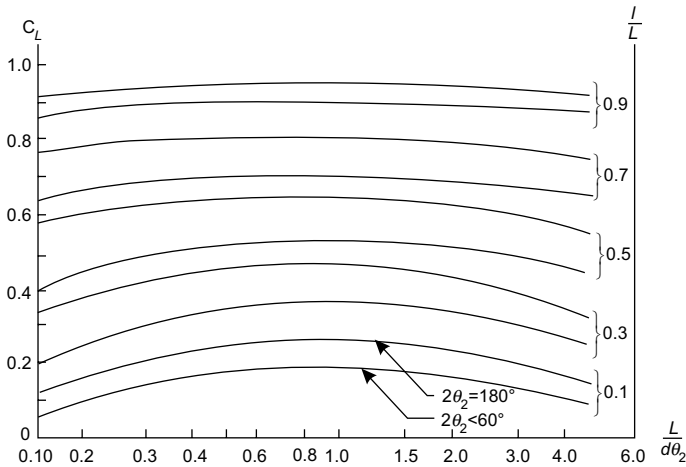

Fig. 5.28 *Load coefficient for a cylindrical pad with rectangular pocket having proportional sill area*

The load capacity P of a hydrostatic journal is found as $P = P_{pr}$. *It may be alternately determined by the procedure discussed below.*

$$p = p_p \cdot A \cdot C_L \cdot C_p(\varepsilon, k) \text{ kgf} \qquad (5.69)$$

which is similar to Eq. (4.63) for closed hydrostatic slideways. In Eq. (5.69), coefficient $C_p(\varepsilon, k)$ depends upon

1. eccentricity ratio $\varepsilon = e/c$, and
2. k, which depends upon the accuracy and surface finish of the spindle.

In high accuracy and precision machine tools in which hydrostatic journal bearings are employed, the load on the journal is small, and hence eccentricity e is also small. For $\varepsilon \leq 0.4$, the value of $C_p(\varepsilon, k) = (3/2)\varepsilon$ can be assumed to be sufficiently accurate for all practical purposes. If the l/d ratio of the bearing is taken equal to unity, the effective area of all the pads $(A \cdot C_L)$ can be taken equal to $0.5d^2$. Upon substituting the above values of $A \cdot C_L$ and $C_p(e, k)$ in Eq. (5.70), we get the following simplified expression for the load capacity of a hydrostatic journal bearing:

$$P = 0.75 \cdot \varepsilon \cdot d^2 \cdot p_p = 0.75 \cdot \frac{e}{c} d^2 p_p \tag{5.70}$$

The stiffness k of a hydrostatic journal bearing is obtained from the expression $K = dP/de$. For small values of eccentricity, we can assume $dP/de \approx P/e$, and therefore, from Eq. (5.70),

$$K = \frac{P}{e} = 0.75 \frac{d^2 p_p}{c} \tag{5.71}$$

A conservative estimate of the oil film stiffness can be obtained from the expression,

$$k \approx \frac{3P}{c} \tag{5.72}$$

The viscosity μ of the lubricant is determined from consideration of minimum frictional loss and it is given by the expression,

$$\mu = 2.2 \times 10^8 \left(\frac{c}{r}\right)^2 \frac{p_p}{n} \text{ cP} \tag{5.73}$$

where c/r = ratio of radial clearance to the journal radius; both c and r are in cm
  n = rpm of the journal
  p_p = supply pressure, kgf/cm^2

The restrictors are, as already explained in Sec. 4.4.2, used to control the rate of flow of lubricant through the bearing gap. The flow through a capillary restrictor is

$$Q_c = \frac{(p_p - p_0)}{R_{rc}} \tag{5.74}$$

and the flow through an orifice restrictor is

$$Q_0 = k_0 \sqrt{2(p_p - p_0)} \tag{5.75}$$

In Eqs (5.74) and (5.75), R_{rc} and k_0 represent the constants of the capillary tube and orifice, espectively. They depend upon the geometrical parameters of the restrictor and the density and absolute viscosity of the lubricant, and are defined by Eqs (4.52) and (4.52'), respectively.

Equations (5.66)–(5.75) are the basic design equations of hydrostatic journal bearings. They can be used for determining pad geometry and dimensions, restrictor parameters, bearing load capacity, etc. depending upon the particular design problem.

5.6.4 Air-lubricated Bearings

The use of high rotational speed in fluid-lubricated bearings is restricted by frictional losses and heat generation in the lubricant. Rotational speeds can be considerably raised by using a lubricant of lower viscosity. This

explains the recent development of using air-lubricated bearings in spindles of some high-speed precision machines. Air has a viscosity which is approximately 100 times less man that of kerosene and more than 1000 times less than that of industrial oil. The main shortcomings that restrict the application of air lubricated bearings are low load capacity and extreme sensitivity to overloading. The slightest over loading breaks the air film, causing direct metal-to-metal contact at high rotating speeds with all the serious repercussions of such an accident. Air-lubricated bearings are made of babbit or other similar anti-friction materials, which permit operation under dry friction conditions, though for an extremely short duration. Air-lubricated bearings can be of two types:

1. Aerodynamic
2. Aerostatic

1. **Aerodynamic Bearings**   These bearings operate on the principle of aerodynamic effect of a spindle floating on an air wedge at high rotational speed. They are used in light spindles which rotate at exceptionally high speeds of the order of $\omega = 10^3$–10^4 rad/s, but are subjected to low pressures—$p \approx 1$ kgf/cm^2. The examples of application of aerodynamic bearings are spindles of internal grinding machines, centrifuges, gyroscopes, gas turbines, etc.

The load capacity of an aerodynamic bearing can be determined as

$$P = 0.5p_a \cdot l \cdot d \cdot K_1 \cdot K_2 \text{ kgf} \tag{5.76}$$

where p_a = air supply pressure, kgf/m^2; generally $p_a = (2$–$5) \, 10^4$ kgf/m^2

   l = length of the bearing, m

   d = diameter of the bearing, m

   K_1, K_2 = coefficients

Coefficient K_1 is a function of the Sommerfeld number. It is plotted in Fig. 5.29 for different values of eccentricity ratio ε.
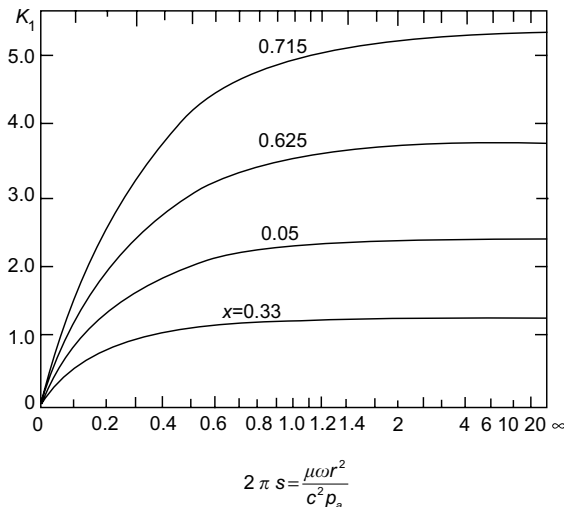

Fig. 5.29   *Design curves for computing K_1 as a function of Sommerfeld number for different values of ε*

Coefficient K_2 depends upon the ratio $l/\eta d$, where η is, in its turn, a function of the Sommerfeld number. The curves $K_2 = f(l/\eta d)$ and $\eta = f(\mu\omega r^2/c^2 p_a)$ are given in Figs 5.30 and 5.31, respectively.

The heat generation in aerodynamic bearings is negligible, and therefore, the check for bearing temperature is not necessary. The air which is supplied to aerodynamic bearings is dehydrated and mixed with a small quantity of oil to avoid corrosion. Also, to avoid jamming of the journal and bearing surfaces at the time of starting or stopping the spindle (when the aerodynamic effect is negligible), air is supplied at a pressure of $(2$–$5)\ 10^4$ kgf/m^2.

2. **Aerostatic Bearings**   As has already been stated above, aerodynamic bearings are used only in spindles rotating at exceptionally high speeds. In the spindles of precision machine tools, aerostatic bearings have found wider application as they can operate satisfactorily at relatively lower rotational speeds also.
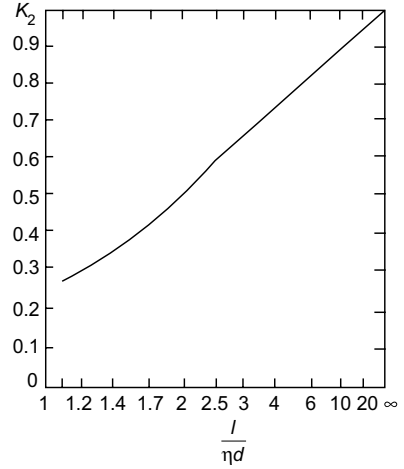

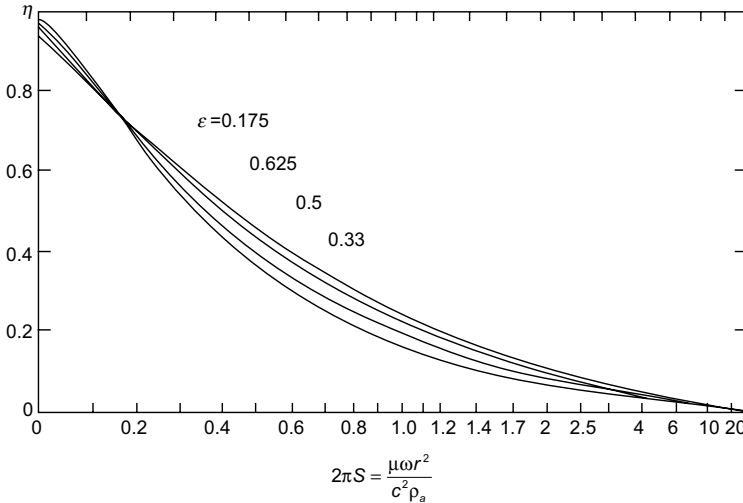**Fig. 5.30**   *Design curve for computing K_2 as a function of $l/\eta d$*

Fig. 5.31   *Variation of η as a function of Sommerfeld number*

The principle of operation of an aerostatic journal bearing is similar to that of a hydrostatic bearing. The schematic diagram of an aerostatic bearing is shown in Fig. 5.32.

Air is supplied at a supply pressure of $p_s = 3$–4 kgf/cm^2. Generally, air is supplied at the ends as shown in Fig. 5.32. However, in short bearings it can be supplied at the middle of the bearing. The air pockets should

be connected by an annular microgroove which is shown in Section *A-A* in Fig. 5.32. The size and shape of the microgroove are selected from the same considerations which were discussed in Sec. 4.5 with reference to aerostatic slideways. The air is fed into the clearance between the bearing and journal through 0.2–0.3 mm holes.
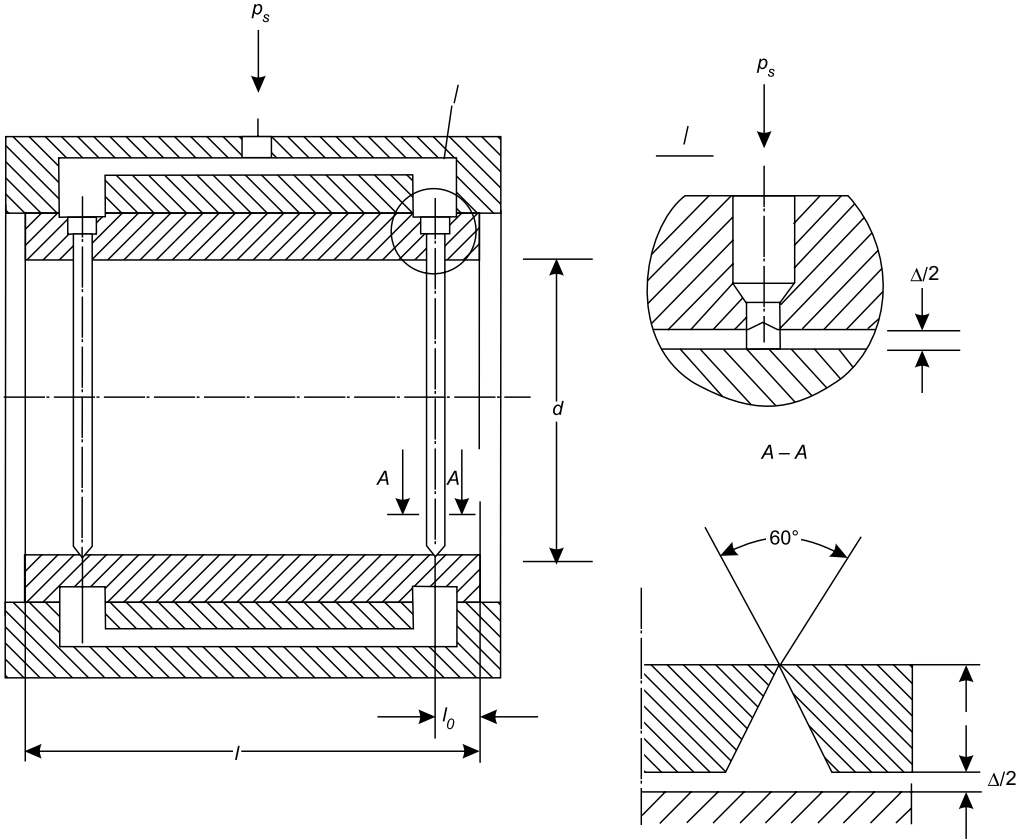

Fig. 5.32   *Schematic diagram of an aerostatic bearing*

The radial clearance is found as

$$c = (0.001 - 0.002)d, \text{ m} \tag{5.77}$$

where d = diameter of the bearing, m

The *number of holes* through which air is supplied is tentatively found from the expression,

$$Z = 20 \cdot \pi \cdot d \tag{5.78}$$

and then rounded off to the nearest higher whole number. Generally, $Z \geq 4$.

The *load capacity* of an aerostatic bearing can be determined from the following relationship:

$$P = 0.12 p_s \cdot d(l - l_0) \cdot C_p(\varepsilon) \tag{5.79}$$

where p_s = air supply pressure, kgf/m^2
    l = length of the bearing, m
    l_0 = distance of the air supply hole from the bearing edge, m
    $C_p(\varepsilon)$ = coefficient, which depends upon the eccentricity ratio

Coefficient $C_p(\varepsilon)$ is given by the following approximate relationship:

$$C_p(\varepsilon) = \frac{\pi}{\varepsilon}[(1 - \varepsilon^2)^{-1/2} - 1] \tag{5.80}$$

Upon expanding the series,

$$(1 - \varepsilon^2)^{-1/2} - 1 = \frac{1}{2}\varepsilon^2 + \frac{3}{8}\varepsilon^4 + \frac{5}{16}\varepsilon^6 + \cdots$$

and neglecting the higher-order terms except the first (which is acceptable for $\varepsilon < 0.3$), the following simple expression for load capacity of aerostatic bearing can be obtained:

$$P = 0.2 \cdot \varepsilon \cdot p_s \cdot d(l - l_0), \text{ kgf} \tag{5.81}$$

Stiffness $K = dP/de$ of the aerostatic bearing can be obtained by substituting $\varepsilon = e/c$ in Eq. (5.81) and differentiating it.

$$K = \frac{dP}{de} \approx \frac{P}{e} = \frac{0.2 p_s \cdot d(l - l_0)}{c} \frac{\text{kgf}}{\text{m}} \tag{5.82}$$

The recommended l/d ratio is

$$l/d = 1 - 1.5 \tag{5.83}$$

Distance l_0 should be taken as

$$l_0 = 0.1l \tag{5.84}$$

Review Questions

5.1 While turning a 750 mm long workpiece of 100 mm diameter between centres, the radial cutting force was found to be 150 kgf when the tool was 200 mm from the tailstock. Calculate the machine tool and system compliances if the stiffness of the saddle, headstock and tailstock is 3000, 4000 and 2500 kgf/mm, respectively.

5.2 During the turning operation on a workpiece held between centres, the tangential cutting force component was 150 kgf and the radial – 80 kgf. If the workpiece is 500 mm long and has diameter = 80 mm, determine the deflection when the tool is 200 mm from the headstock. The headstock and tailstock stiffness is 35,000 and 15,000 kgf/cm, respectively.

5.3 A solid steel spindle (*see* Fig. 5.5a) transmits a torque of 40 kgf · m through a gear of module 3 mm and number of teeth 80. Ratio $a/b = 2$ and compliances of front and rear bearings are 0.1 and 0.15 micron/kgf, respectively. Determine the optimum l/c ratio to ensure minimum deflection of the spindle nose if force $P_1 = 150$ kgf.

5.4 Determine the outer and inner diameters of a hollow lathe spindle if their ratio = 2. The power on the spindle is 4.5 kW and it is rotating at 700 rpm. The peripheral and radial forces on the spindle are P_2 = 215 kgf and T_2 = 78 kgf. A horizontal force P_1 = 210 kgf and a vertical force T_1 = 60 kgf are acting on the spindle nose. The spindle dimensions and loading are shown in Fig. 5.33.
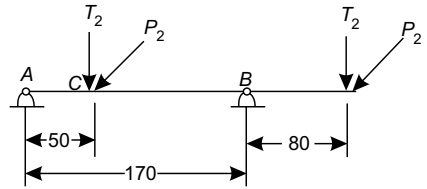

Fig. 5.33 *Schematic diagram of a lathe spindle*

5.5 The spindle of a high-speed precision lathe has a diameter 80 mm and can run at a speed up to 2500 rpm. Select a suitable sleeve-bearing material for the above spindle if the maximum load on the bearing = 30 kgf and the length-to-diameter ratio of the journal = 1.

5.6 Select the design parameters of a full hydrodynamic journal bearing of copper-lead alloy for a journal of 60 mm diameter to support a load of 150 kgf at 3000 rpm. Assume h_{cr} = 10 microns and h_{min}/h_{cr} > 1.1.

5.7 Design a full hydrodynamic babbit bearing for a journal of diameter 80 mm rotating at 2000 rpm. Determine its load capacity if the average bearing pressure is not to exceed 8 kgf/cm². Check the bearing against excessive heating if the maximum permissible bearing temperature is 70°C and the maximum ambient temperature = 40°C.

5.8 Design a multiple-wedge hydrodynamic bearing for a grinding machine if the journal diameter = 60 mm and it rotates at 3000 rpm. What is the load capacity of the unloaded bearing? How much load can the bearing support when the eccentricity ratio = 0.7? Also, determine the flow rate of the lubricant if the operating temperature of the lubricant is 85°C. The lubricant has a kinematic viscosity = 6 cS, density = 0.86 g/cm³ and specific heat = 0.4 kcal/kg · °C.

5.9 A cylindrical pad hydrostatic bearing having r/R ratio = 0.7 (*see* Fig. 5.24) supports a load of 200 kgf at 1000 rpm. The bearing is fed through an orifice restrictor having discharge coefficient = 0.6. Determine the required restrictor opening if the pump pressure = 20 kgf/cm², minimum film thickness = 0.005 cm and absolute viscosity of the lubricant = 4×10^{-7} kgf · s/cm².

5.10 Determine the length and diameter of an aerodynamic bearing to support a load of 15 kgf. Given l/d = 0.8, air supply pressure = 4 kgf/cm², radial gap = 0.01 mm and absolute viscosity of air = 0.02 cP.

5.11 A CI bar (BHN = 200) Φ 75 × 500 is reduced to Φ 73 on a lathe by a turning tool placed at the tail stock end at s = 0.23 mm/rev. Compliance of the head stock, saddle and tailstock is 0.25, 0.25 and 0.3 microns/kgf, respectively. Given $Py = 88\ t^{0.9}s^{0.75}$ kgf. Calculate the true depth of cut.

5.12 A machine spindle is supported on two anti-friction bearings 20 cm apart and having radial clearances of 4 and 6 microns, respectively. Determine the radial run out of the spindle nose if its overhang is 8 cm from the bearing having 6 micron clearance.

References

1. Levina, ZM, *et al.*, "Investigation of the stiffness of tapered joints", *Stanki I Instrument*, 1973, No. 10.
2. Kuvshinskii, VV, *Milling Operation*, Mashinostroenie Publishers, Moscow, 1977, p. 127
3. Mamet, OP, *Concise Handbook of Machine Tool Design*, Mashinostroenie Publishers, Moscow, 1964, p. 186.

4. Elyashev, A, "Fundamentals of machine tool design", *Notes for UNIDO Course*, Moscow, p. 80.
5. Ibid., p. 82.
6. Honrath, K, *Werkzengmaschinenspindeln und Deren Langerungev*, T.H. Aachen, Ind Anz, 1957,
7. Sokolov, Yu N, "Multiple-wedge hydrodynamic bearings of precision machine tool spindles", *Stanki I Instrument*, 1963, No. 8.
8. Rippel, HC, *Cast Bronze Hydrostatic Bearing Design Manual*, Cast Bronze Bearing Institute, Inc., 1963.